The mucinous domain of pancreatic carboxyl-ester lipase (CEL) contains core 1/core 2 *O*-glycans that can be modified by ABO blood group determinants

Received for publication, January 23, 2018, and in revised form, September 11, 2018 Published, Papers in Press, October 12, 2018, DOI 10.1074/jbc.RA118.001934

Khadija El Jellas,[a,b,c] Bente B. Johansson,[c,d,1] Karianne Fjeld,[c,e,1] Aristotelis Antonopoulos,[f] Heike Immervoll,[a,g] Man H. Choi,[a,b] Dag Hoem,[h] Mark E. Lowe,[i] Dominique Lombardo,[j] Pål R. Njølstad,[c,d] Anne Dell,[f] Eric Mas,[j] Stuart M. Haslam,[f] and Anders Molven[a,b,c,2]

From the [a]Gade Laboratory for Pathology, Department of Clinical Medicine, University of Bergen, N-5020 Bergen, Norway, [b]Department of Pathology, Haukeland University Hospital, N-5021 Bergen, Norway, [c]KG Jebsen Center for Diabetes Research, Department of Clinical Science, University of Bergen, N-5020 Bergen, Norway, [d]Department of Pediatrics and Adolescent Medicine, Haukeland University Hospital, N-5021 Bergen, Norway, [e]Center for Medical Genetics, Haukeland University Hospital, N-5021 Bergen, Norway, [f]Department of Life Sciences, Imperial College London, South Kensington Campus, London SW7 2AZ, United Kingdom, [g]Department of Pathology, Ålesund Hospital, N-6017 Ålesund, Norway, [h]Department of Gastrointestinal Surgery, Haukeland University Hospital, N-5021 Bergen, Norway, [i]Department of Pediatrics, Washington University School of Medicine, St. Louis, Missouri 63110, and [j]INSERM, CRO2, Center for Research in Biological Oncology and Oncopharmacology, Aix-Marseille University, 13284 Marseille Cedex 07, France

Edited by Qi-Qun Tang

Carboxyl-ester lipase (CEL) is a pancreatic fat-digesting enzyme associated with human disease. Rare mutations in the *CEL* gene cause a syndrome of pancreatic exocrine and endocrine dysfunction denoted MODY8, whereas a recombined *CEL* allele increases the risk for chronic pancreatitis. Moreover, CEL has been linked to pancreatic ductal adenocarcinoma (PDAC) through a postulated oncofetal CEL variant termed feto-acinar pancreatic protein (FAPP). The monoclonal antibody mAb16D10 was previously reported to detect a glycotope in the highly *O*-glycosylated, mucin-like C terminus of CEL/FAPP. We here assessed the expression of human CEL in malignant pancreatic lesions and cell lines. CEL was not detectably expressed in neoplastic cells, implying that FAPP is unlikely to be a glycoisoform of CEL in pancreatic cancer. Testing of the mAb16D10 antibody in glycan microarrays then demonstrated that it recognized structures containing terminal GalNAc-α1,3(Fuc-α1,2)Gal (blood group A antigen) and also repeated protein sequences containing GalNAc residues linked to Ser/Thr (Tn antigen), findings that were supported by immunostainings of human pancreatic tissue. To examine whether the CEL glycoprotein might be modified by blood group antigens, we used high-sensitivity MALDI-TOF MS to characterize the released *O*-glycan pool of CEL immunoprecipitated from human pancreatic juice. We found that the *O*-glycome of CEL consisted mainly of core 1/core 2 structures with a composition depending on the subject's *FUT2* and *ABO* gene polymorphisms. Thus, among digestive enzymes secreted by the pancreas, CEL is a glycoprotein with some unique characteristics, supporting the view that it could serve additional biological functions to its cholesteryl esterase activity in the duodenum.

Carboxyl-ester lipase (CEL)[3] (EC 3.1.1.13), also designated bile salt–dependent lipase, is one of four major duodenal lipases secreted by pancreatic acinar cells (1). In addition, mammalian breast glands secrete CEL, alternatively called bile salt–stimulated lipase, into mother's milk (2). CEL is involved in the hydrolysis and absorption of dietary fat, cholesteryl esters, and fat-soluble vitamins. It constitutes a significant fraction of pancreatic juice, around 4% of the total protein content (3).

The 11 exons of the *CEL* gene code for a short signal peptide and a globular N-terminal domain of 535 amino acid residues in which the bile salt–binding site and the catalytic activity of the enzyme reside (4). The last exon contains a variable number of tandem repeats (VNTR) that give rise to a flexible C terminus protruding from the globular core (5). The VNTR encodes 11–amino acid segments that are repeated from 3 to 23 times in humans (6), with16 repeats being the most common number (7–9). The variable length of the *CEL* VNTR makes this gene and its protein product highly polymorphic in human populations. In particular, rare mutational events affecting the VNTR region cause an inherited syndrome of diabetes and pancreatic exocrine dysfunction (MODY8) (10), most likely because of protein aggregation and endoplasmic reticulum stress resulting

This work was supported by Ph.D. fellowship 911831 (to K. E. J.) and Research Grant 912057 (to A. M.) from Western Norway Regional Health Authority (Helse Vest). The work was also supported by grants from the Gade Legacy (to K. E. J.), Stiftelsen Kristian Gerhard Jebsen (to P. R. N.), Research Council of Norway's FRIMEDBIO Program (to A. M.), and by Biotechnology and Biological Sciences Research Council Grant BB/K016164/1 (to A. D. and S. M. H.). The authors declare that they have no conflicts of interest with the contents of this article.

This article contains Figs. S1–S4 and Table S1.

[1] These authors contributed equally to this work.

[2] To whom correspondence should be addressed: Dept. of Pathology, Haukeland University Hospital, N-5021 Bergen, Norway. Tel.: 47-55973169; E-mail: anders.molven@uib.no.

[3] The abbreviations used are: CEL, carboxyl-ester lipase; VNTR, variable number of tandem repeats; FAPP, feto-acinar pancreatic protein; PDAC, pancreatic ductal adenocarcinoma; ADM, acinar-to-ductal metaplasia; PanIN, pancreatic intraepithelial neoplasia; RT-qPCR, real-time quantitative PCR; FFPE, formalin-fixed paraffin-embedded; RIPA, radioimmune precipitation assay buffer.

from altered repeat sequences (11–13). Moreover, a recombined allele between the VNTR regions of CEL and the neighboring pseudogene *CELP* is associated with a significantly increased risk for chronic pancreatitis (14, 15).

The mature form of CEL is heavily glycosylated. Its globular domain contains a *N*-linked glycan at the conserved residue Asn-210 (16–18), whereas the VNTR domain has a high occupation of *O*-linked glycans on its threonine, and probably serine, residues (16, 19), similar to that found in mucinous glycoproteins (20). As a consequence of the VNTR length variability and possible differences in the glycan pool, the molecular mass of the CEL glycoprotein may span from 60 to 140 kDa (7, 11).

Glycosylation changes are a hallmark of disease, especially prominent in inflammation and cancer (21). Some studies have indirectly implicated glycovariants of CEL in malignant disease by using antisera against embryonic pancreas extracts to search for acinar cell factors that are absent in the adult pancreas and re-expressed during oncogenesis (22, 23). Among many antibodies produced against fetal pancreatic tissue, the antibody mAbJ28 detected a concanavalin A–reactive pancreatic glycoprotein with estimated molecular mass of 110 kDa (24). This acinar cell component was given the name feto-acinar pancreatic protein (FAPP) (24, 25). FAPP was later reported to have the same amino acid composition as the N-terminal globular domain of CEL (26) and postulated to be a CEL variant expressed in embryogenesis, inflammation, and cancer. However, whether oncofetal forms of CEL exist has not been confirmed.

Another antibody that seemingly targets a CEL-related glycotope on FAPP is mAb16D10. This monoclonal antibody was raised against CEL purified from pancreatic juice of a PDAC patient (27). In SOJ-6 pancreatic cancer cells, mAb16D10 has been found to specifically recognize an antigen present on the plasma membrane (28), to inhibit the growth of tumor xenografts (28), and to induce cell death by the p53/caspase-dependent apoptotic pathway (27). In human pancreatic tissue sections, mAb16D10 was reported to discriminate pancreatic cancer from nonneoplastic tissue and other cancers (29).

We sought to confirm and further characterize the postulated onco-glycoforms of CEL by 1) evaluating human CEL expression in PDAC surgical specimens, 2) determining the identity of the 16D10 glycotope by means of glycan arrays, and 3) identifying the *O*-glycan structures at the CEL mucinous tail by means of high-sensitivity MALDI-TOF MS. However, we could not detect CEL expression in neoplastic cells and found that mAb16D10 did not target an epitope specific for CEL or for pancreatic cancer tissue. Instead, the antibody showed a high affinity for blood group A antigens, which led to the finding that ABO blood group determinants are present on the C terminus of CEL.

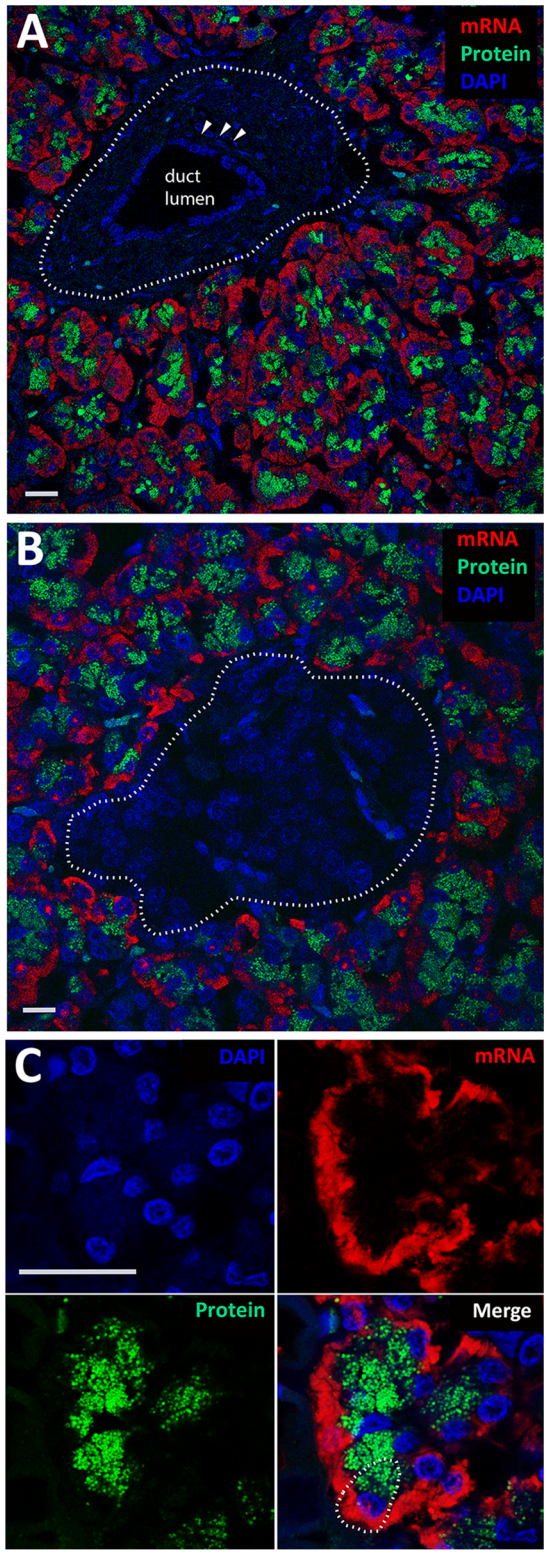

Figure 1. CEL expression in the pancreas is restricted to acinar cells. *A*, double fluorescent labeling of CEL mRNA (*red*) and protein (*green*) in normal human pancreatic parenchyma. Acinar cells are strongly positive, whereas ductal cells are negative. The *dotted line* circumscribes a representative intralobular duct. *White arrowheads* indicate the epithelial lining of the duct lumen. *B*, a representative islet of Langerhans (circumscribed by *dotted line*) devoid of CEL expression. *C*, high magnification of an acinus with one well-polarized acinar cell highlighted by the *dotted line*. Note the basal labeling of the mRNA and the apical position of the zymogen granules staining positive for CEL protein. Cell nuclei are stained *blue* with DAPI. A single z-plane is shown (0.19 μm). *Scale bars* represent 100 μm.

Results

CEL expression in normal pancreas, PDAC, and pancreatic cancer cell lines

Initially, we performed fluorescent *in situ* hybridization and immunohistochemistry for simultaneous detection of CEL mRNA and protein, respectively, in morphologically normal

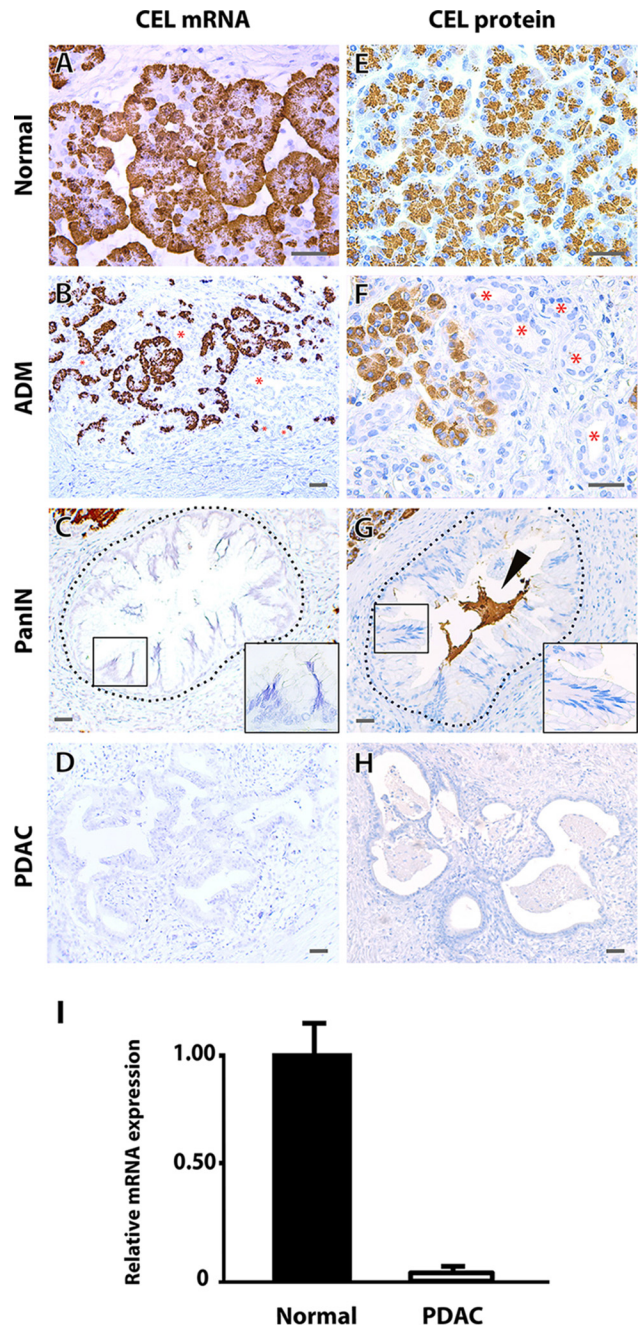

Figure 2. Pancreatic premalignant and malignant lesions are negative for CEL expression. *A–D,* chromogenic *in situ* labeling of CEL mRNA in sections from representative pancreatic cancer cases. *E–H*, chromogenic immunostaining of CEL protein in adjacent sections of *A–D*. *A* and *E*, preserved pancreatic parenchyma with normal morphology. Acinar cells contain high levels of CEL mRNA and protein located basally and apically, respectively. *B* and *F*, areas of atrophy with ADM (marked by *red asterisks*). Both CEL mRNA and protein cease to be expressed when a lumen is visible. *C* and *G*, a PanIN lesion (circumscribed by *dotted line*). *Insets*, magnification of one papillary protrusion showing negative epithelial cells. The *arrow* in *G* indicates secreted CEL protein present in the duct lumen. *D* and *H*, malignant pancreatic ducts embedded in desmoplastic stroma. All structures in these areas were devoid of detectable levels of both CEL mRNA and protein. *Scale bars* in *A–H* represent 100 μm. *I*, RT-qPCR comparing *CEL* transcript level in PDAC sections (areas corresponding to *D*/*H*; $n = 9$ different patients) with level in normal pancreatic tissue from patients with nonpancreatic pathologies ($n = 4$). *QARS* gene expression was used as normalizing control. Values are expressed as mean ± S.E.

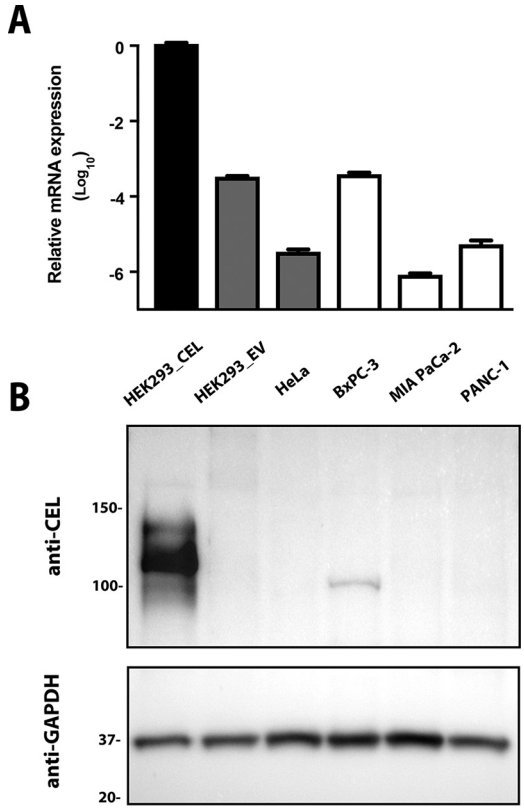

Figure 3. CEL expression is low or absent in pancreatic cancer cell lines. *A*, *CEL* mRNA levels of the pancreatic cancer cell lines BxPC-3, MIA PaCa-2, and PANC-1 compared with levels in HeLa cells and in stably transfected HEK293 cells (positive control: HEK293_CEL, transfected with a CEL-expressing plasmid construct; negative control: HEK293_EV, transfected with empty plasmid vector). *GAPDH* gene expression was used as loading control. *y*-Axis scale is logarithmic. *Error bars* represent S.D. from three experimental replicates. *B*, a representative Western blot ($n = 2$) of protein lysates from the above cell lines stained with anti-CEL antibody. GAPDH protein levels in the *lower panel* was used as loading control.

pancreas (Fig. 1). Our staining method did not detect CEL transcripts or protein in ductal cells or in islets of Langerhans (Fig. 1, *A* and *B*). The acinar cells were strongly positive, as expected, with CEL transcripts located basally and the protein accumulating apically in the zymogen granules (Fig. 1*C*). Having established the specificity of our method, we evaluated CEL mRNA and protein expression in adjacent sections from PDAC tumors by chromogenic staining (Fig. 2). CEL was detectable in preserved and atrophic parenchyma (Fig. 2, *A*, *B*, *E*, *F*). In contrast, the epithelial lining of acinar-to-ductal metaplasia (ADM), pancreatic intraepithelial neoplasia (PanIN), and malignant ducts were consistently negative (Fig. 2, *B–D* and *F–H*).

Next, RT-qPCR was performed on selected areas of unstained pancreatic FFPE sections, which were scraped off the glass slide after comparison with H&E-stained parallel sections. Neoplastic regions from nine different PDAC patients were compared with morphologically normal regions from four patients having nonneoplastic disease. Very low *CEL* mRNA levels were detected in the neoplastic areas compared with levels in normal pancreatic parenchyma (Fig. 2*I*). In addition, the commonly used pancreatic cancer cell lines BxPC-3, MIA PaCa-2, and PANC-1 were tested for CEL expression (Fig. 3*A*). MIA PaCa-2 and PANC-1 exhibited very low mRNA levels

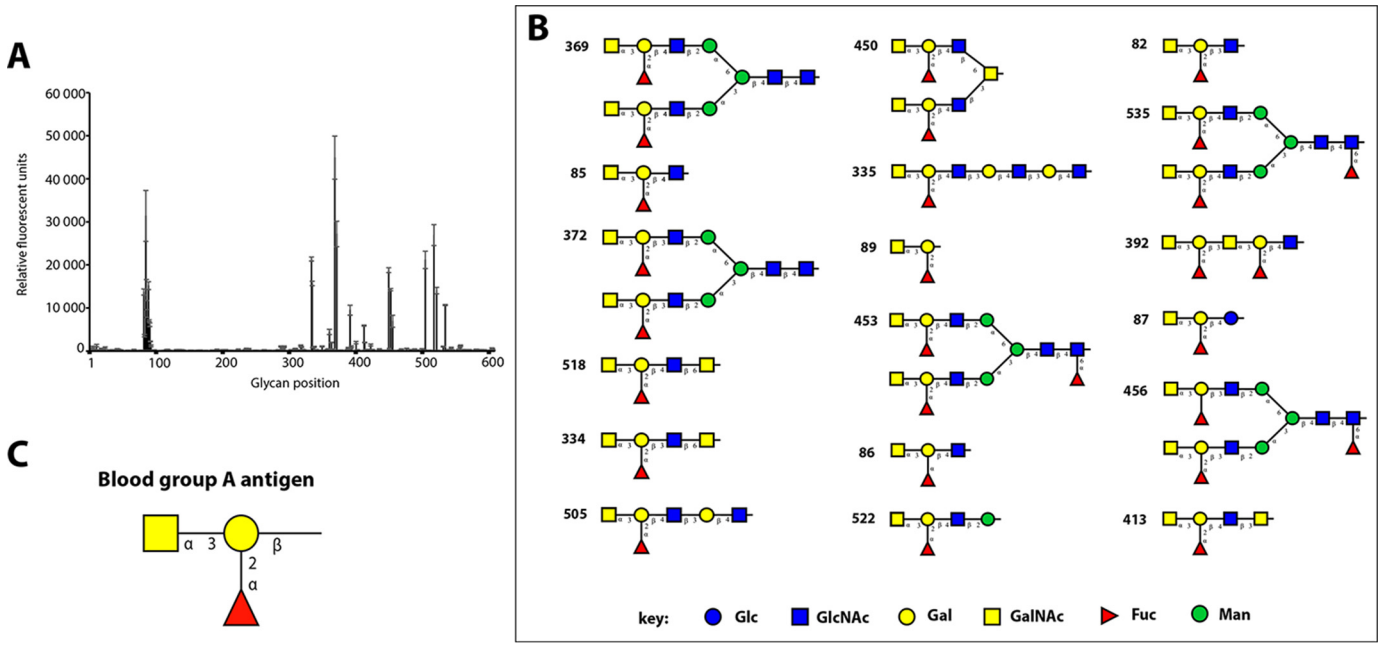

Figure 4. The mAb16D10 antibody binds strongly to blood group A–containing structures in a glycan array. *A*, mAb16D10 screened against 609 different glycans on a printed microarray from the Consortium for Functional Glycomics (see "Experimental procedures"). Binding was detected via Alexa Fluor 488–labeled anti-mouse secondary antibody. *B*, the 18-glycan structures with the highest affinity shown in decreasing order of binding. *Numbers* refer to position in the array in *A*. *C*, the structural motif common to all binding structures. This was the terminal glycan having the sequence GalNAc-α1,3(Fuc-α1,2)Gal-, which corresponds to the blood group A antigen.

(comparable to the basal levels in HeLa cells). BxPC-3 cells had a CEL mRNA level comparable with that of native HEK293 cells. Immunoblots stained with an anti-CEL antibody detected a strong protein band in the control HEK293_CEL line and a weak band in BxPC-3 cells, but no signal in the other cell lines (Fig. 3*B*).

Characterization of the 16D10 glycotope

The mAb16D10 antibody had been produced against purified CEL (27) and was shown to react well with pancreatic cancer tissue sections (29). Because we did not detect CEL mRNA or protein in neoplastic cells of PDAC tumors, we next sought an explanation for the reactivity of the mAb16D10 antibody. To this end, an aliquot of mAb16D10 was analyzed on a glycan microarray (see "Experimental procedures"). By comparing bound and unbound structures, we concluded that mAb16D10 had a strong reactivity toward the structural motif GalNAc-α1,3(Fuc-α1,2)Gal, which corresponds to the blood group A antigen (Fig. 4). To verify this result, the antibody was used to stain normal pancreatic parenchyma from subjects of blood group A and O. There was strong positivity toward normal acinar cells from individuals with blood group A, but not in blood group O pancreatic tissue (Fig. S1, *A* and *C*). Similarly, mAb16D10 specifically stained both erythrocytes and endothelium of blood group A, but not O specimens (Fig. S1, *B* and *D*).

We then examined the reactivity of mAb16D10 on pancreatic tissue sections from PDAC cases of different ABO phenotypes. Blood group A cases exhibited a virtually identical staining pattern when parallel sections were incubated with either anti-A antibody or mAb16D10 (Fig. 5, *A–H)*. There was strong reactivity with acinar cells, ducts, blood vessels, and red blood cells in areas of preserved morphology (Fig. 5, *A* and *E*), as well

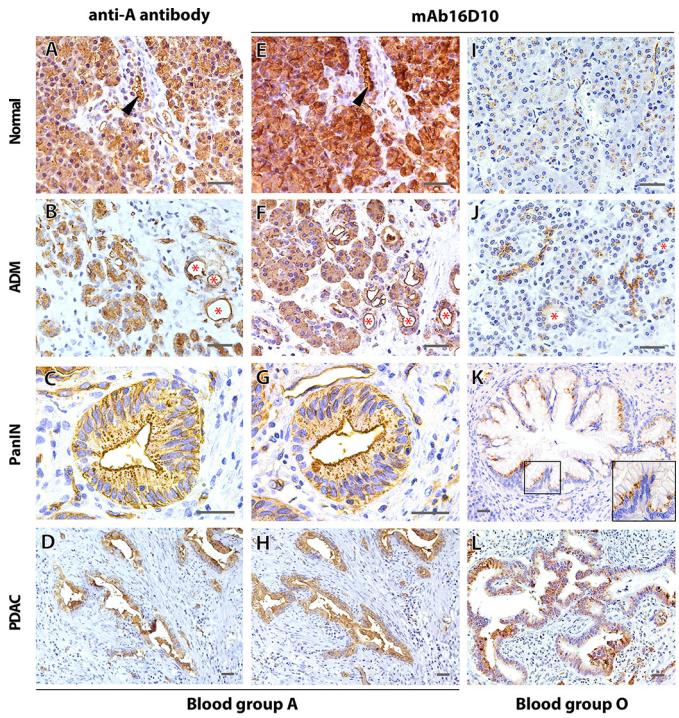

Figure 5. The mAb16D10 antibody cross-reacts with blood group A antigens in pancreatic cancer tissue. *A–H*, adjacent tissue sections from a patient with blood group A immunostained either with mAb16D10 or an anti-A antibody. *I–L*, tissue sections from a patient with blood group O immunostained with mAb16D10. *A*, *E*, and *I*, preserved pancreatic parenchyma with normal morphology. The *arrowhead* points to pancreatic secretions within a small duct. *B*, *F*, and *J*, areas of atrophy with acinar-to-ductal metaplasia (ADM, marked by *red asterisks*). *C*, *G*, and *K*, PanIN lesions. *Inset* in *K*, magnification of one papillary protrusion. *D*, *H*, and *L*, malignant pancreatic ducts embedded in desmoplastic stroma. *Scale bars* represent 100 μm.

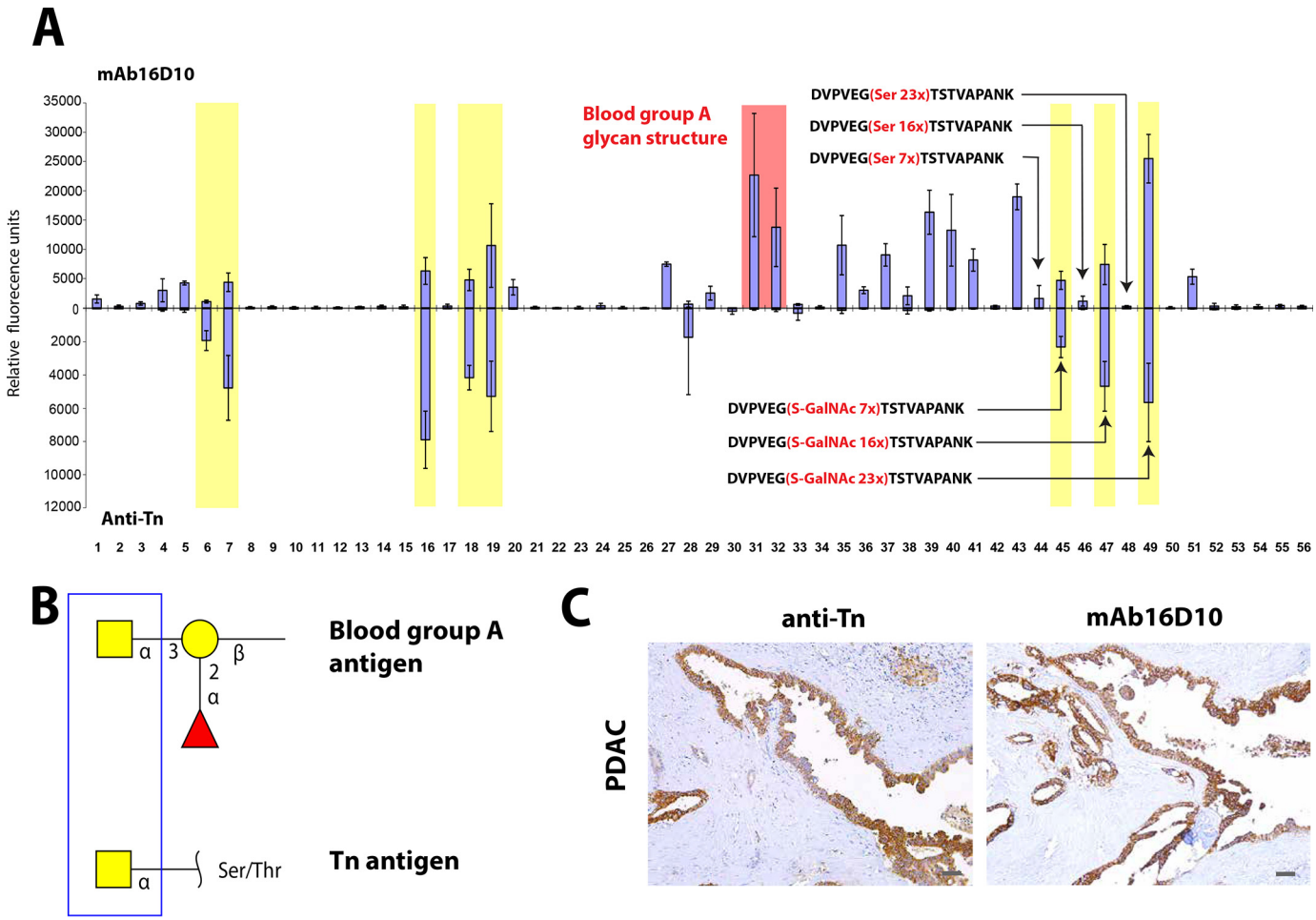

Figure 6. The mAb16D10 antibody can recognize the cancer-associated Tn antigen. *A*, comparative binding profile of mAb16D10 (*upper part*) and an anti-Tn antibody (*lower part*) on an array of synthetic Tn glycopeptides from the Consortium for Functional Glycomics (see "Experimental procedures"). The array consisted of 56 compounds including the blood group A glycan structure (*red box*). Structures that bound both antibodies are highlighted by *yellow boxes*. Only mAb16D10 bound to blood group A antigen structures with high affinity. Note that peptides containing the sequence DVPVEG(S_n)TSTVAPANK showed increasing binding intensities as the number of GalNAc-conjugated serine residues was increased (array positions 45, 47, 49), whereas the same peptide sequences devoid of the sugar bound very weakly (positions 46, 48, 50). Compounds on the array and their binding affinities are listed in Table S1. *B*, the terminal GalNAc-α residue shared by the Tn (GalNAc-α-Ser/Thr) and blood group A (GalNAc-α1,3(Fuc-α1,2)Gal) antigens. *C*, immunostaining with an anti-Tn antibody or mAb16D10 in adjacent sections of malignant pancreatic ducts embedded in desmoplastic stroma (blood group O individual). *Scale bar* represents 100 μm.

as with epithelial cells of ADM, PanIN, and malignant ducts (Fig. 5, *B–D* and *F–H*). However, mAb16D10 also stained sections from PDAC patients with blood group O. Weak positivity, in a dotlike apical pattern, was observed in normal-looking acinar cells close to the tumor area (Fig. 5*I*). When ADM was present nearby, expression of the mAb16D10 glycotope seemed to increase in the small intralobular ducts connecting the acini (Fig. 5*J*). Relatively strong positivity was observed in PanINs and malignant ducts (Fig. 5, *K* and *L*).

Based on the observed staining pattern in blood group O neoplastic tissue (Fig. 5*L*), it was clear that mAb16D10 also recognized some non-A epitope(s). Thus, to further characterize its specificity, mAb16D10 was tested on a second microarray, consisting of peptides with a varying number of GalNAc residues conjugated to Ser or Thr residues (Fig. 6). Among GalNAc-containing peptides, the intensity of the binding increased as the number of GalNAc-α-Ser residues increased, indicating that mAb16D10 bound strongly to repeating poly-Ser-α-GalNAc residues (Fig. 6*A*). Blood group A antigen bears similarity to the cancer-associated Tn antigen as they both carry a terminal GalNAc-α residue (Fig. 6*B*). The glycan array experiment was therefore repeated using an anti-Tn antibody. A certain overlap between the reactivity of this antibody and that of mAb16D10 was indeed observed (Fig. 6*A*). We therefore assumed that mAb16D10 could recognize the Tn antigen in cancerous tissue, and parallel staining of PDAC sections for these two antigens showed very similar patterns in blood group O specimens (Fig. 6*C*). Moreover, we also found that mAb16D10 reacted with gastric and breast cancer tissue sections from blood group O individuals (Fig. S2).

mAb16D10 reactivity in pancreatic juice

We were now left with the conundrum that mAb16D10 recognized the blood group A antigen very well, despite being produced against purified CEL from pancreatic juice. The most straightforward explanation would be that CEL, being a heavily *O*-glycosylated protein (30), can be decorated with blood group

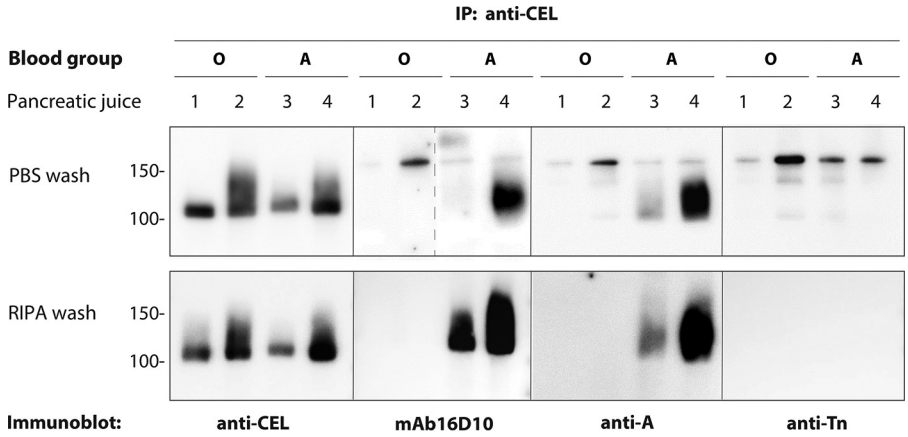

Figure 7. Immunoprecipitated CEL protein from pancreatic juice reacts with mAb16D10 and an anti-A antibody but not with anti-Tn. Co-immunoprecipitation (*upper panel*) and immunoprecipitation (*lower panel*) of CEL were performed on four juice samples, followed by parallel immunoblotting with anti-CEL, mAb16D10, anti-A, or anti-Tn antibodies. CEL was detected at around 110 kDa in all samples. The mAb16D10 and anti-A antibodies gave the same staining pattern in samples from blood group A cases (*juices 3 and 4*). Tn did not react with CEL but showed reactivity toward a protein of higher molecular mass regardless of blood group (*upper panel*). Two different anti-CEL antibodies were used: the mouse mAb As20.1 for immunoprecipitation and a rabbit polyclonal antibody (13) for immunoblotting. The *dashed line* indicates that the membrane part to the left was cut and exposed for a longer time to achieve better signals.

A antigens, which then had stimulated mAb16D10 production. To investigate this hypothesis, we performed immunoprecipitation of CEL directly from pancreatic juice collected from pancreatic cancer patients of either blood type A or O. All four patients had functioning α1,2-fucosyltransferase (as determined by their *FUT2* genotype) and were therefore able to synthesize the H antigen of the ABO blood group system on secreted glycoproteins. Such subjects are referred to as secretors and compose 80% of the Caucasian population (31, 32).

The immunoprecipitated complexes were subjected to SDS-PAGE and immunoblotted with anti-CEL, mAb16D10, and anti-A and anti-Tn antibodies. We performed two experiments, one where the immunoprecipitates were washed with PBS only (Fig. 7, *upper panel*) and another where more stringent washings with RIPA buffer were performed, aiming at dissociating possible complexes that CEL might form with other proteins (Fig. 7, *lower panel*). The anti-CEL antibody detected the protein in all samples as a band of around 110 kDa. After staining with mAb16D10 or anti-A antibody, a band of similar size was detected in blood group A samples but not in samples from blood group O individuals (Fig. 7). This observation strongly supported that CEL could contain terminal blood group A antigens. Anti-Tn staining was negative with regard to detecting a band that corresponded to CEL in molecular size. A high-molecular-mass band at ~170 kDa was seen for all antibodies except anti-CEL, but only when mild washing was applied (Fig. 7, *upper panel*). This might indicate that a CEL-binding protein is present in pancreatic juice and that this protein contains structures with terminal α-GalNAc residues recognizable by all three antibodies.

Characterization of the O-glycome of CEL

Finally, we attempted to detect blood group A epitopes directly on CEL after immunoprecipitation from pancreatic juice. The protein band at 110 kDa (Fig. 7) was excised. As quality control, a small fraction of this band was used for protein identification by MS after trypsin-cleaved peptides/glycopeptides had been extracted. CEL was the major protein species identified (data not shown). Then, MS profiling of *O*-glycans in the excised band was performed using MALDI-TOF-TOF after β-reductive elimination.

The CEL *O*-glycome was analyzed in three samples (Fig. 8): two *FUT2*-positive cases (secretors) of blood group O and A, respectively, and one *FUT2*-negative case (nonsecretor) of blood group O. The latter subject contained a mutation in the *FUT2* gene that leads to a nonfunctional α1,2-fucosyltransferase, meaning that there are no H antigens on secreted glycoproteins to be further converted into A and B antigens. As described below, the identified *O*-glycan pool was in all three cases consistent with *ABO* and *FUT2* genotyping of genomic DNA extracted from the patients' blood samples (32).

The blood group O/secretor sample (Fig. 8*A*) was dominated by the molecular ion *m*/*z* 708 which is consistent with a blood group O antigen (or H antigen) core 1 structure. Core 2 structures containing the H antigen were also seen with a single (*m*/*z* 1158, 1332, and 1519) or two or more LacNAc units (*m*/*z* 1607, 1781, 1968, 2056, and 2230) with or without sialic acid (NeuAc) capping. In the blood group A/secretor sample (Fig. 8*B*), the two highest peaks corresponded to the molecular ion at *m*/*z* 953, which is consistent with a core 1 blood group A structure, and its precursor at *m*/*z* 708 (H antigen). A higher molecular mass structure containing one blood group A antigen on each antenna was detected at *m*/*z* 1822. LacNAc extensions of two units or more were not seen in this sample.

When CEL was isolated from the pancreatic juice of a nonsecretor patient (Fig. 8*C*), the glycan pool lacked the molecular ion *m*/*z* 708. As a consequence, the Gal residue of the precursor Gal-β1,3-GalNAc (*m*/*z* 534, not detected) could only undergo sialylation and therefore *m*/*z* 895 (monosialylated) and 1257 (disialylated) were the two most abundant structures. Core 2 structures were also seen at *m*/*z* 983, 1344, 1433, 1519, 1607, 1794, 1882, and 1968. Fucoses were only part of core 2 structures (*m*/*z* 1519, 1607, and 1968) attached most likely to a GlcNAc residue.

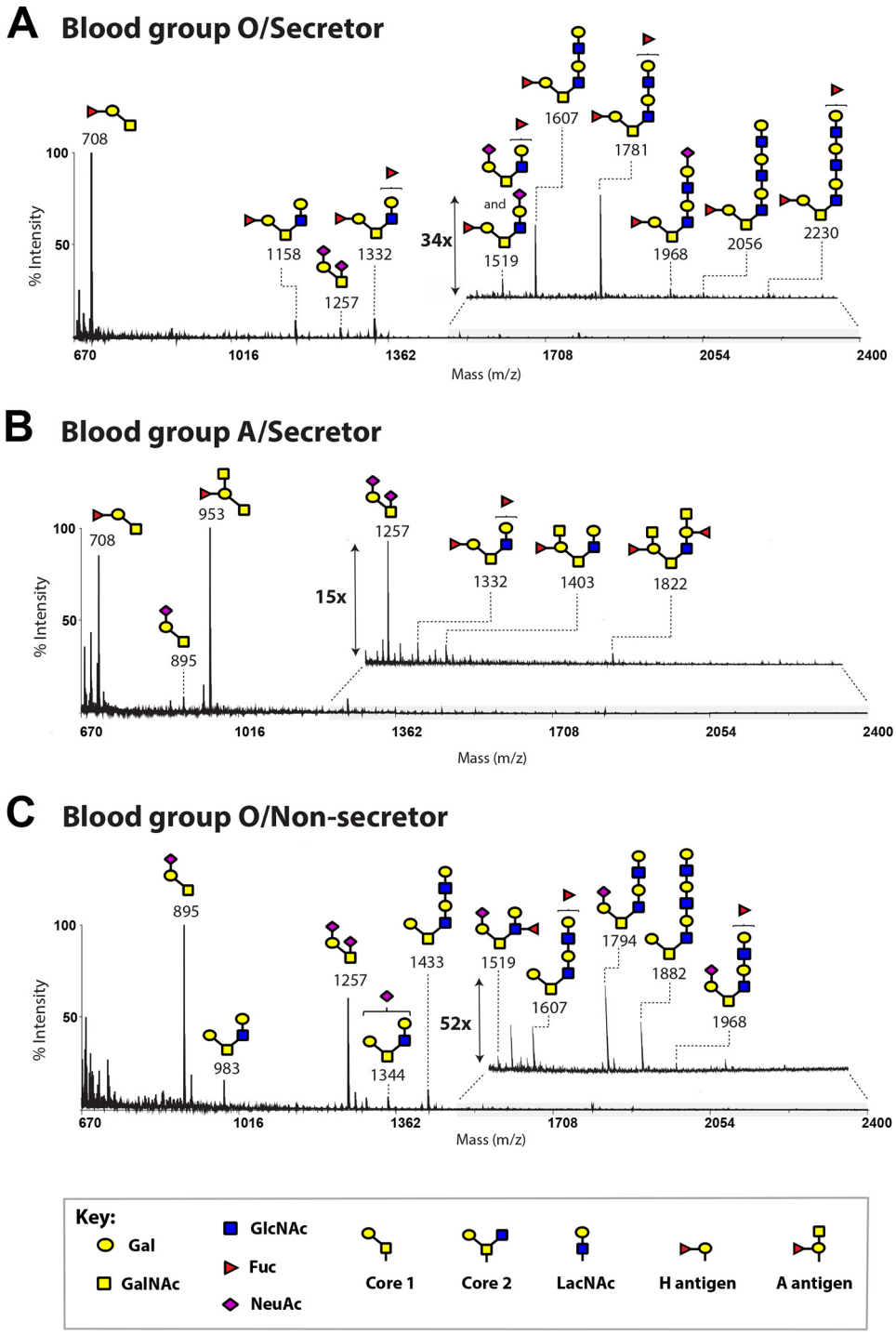

Figure 8. The mucinous domain of CEL contains glycans reflecting the patients' *ABO* and *FUT2* status. The *O*-glycan pool from the pancreatic juice of three PDAC cases was investigated by MALDI-TOF MS after alkaline β-elimination and permethylation. The *O*-glycan population was composed of core 1 and core 2 structures. *A,* spectrum showing *O*-linked glycans from a blood group O *FUT2*-positive (secretor) case. *Inset*, 34× magnification in the *m/z* range 1500–2400 showing core 2 extended structures of less abundance. *B*, corresponding spectrum from a blood group A *FUT2*-positive (secretor) case, with 15× magnification in the *m/z* range 1190–2400. *C*, corresponding spectrum from a blood group O *FUT2*-negative (nonsecretor) case, with a 52× magnification in the *m/z* range 1500–2400. All molecular ions are present in singly charged sodiated form ($[M+Na]^+$). Major peaks are annotated with their proposed carbohydrate structure, according to the symbolic nomenclature adopted by the CFG (66). Putative structures are based on monosaccharide composition, data from the MS/MS analysis of all molecular ions and knowledge of the biosynthetic pathways for *O*-linked glycans. MS and MS/MS spectra were annotated manually with the aid of the semi-automated tool GlycoWorkbench (65). When structures have not been unequivocally defined from MS/MS information, the monosaccharide is shown after a bracket.

Structural assignment was facilitated by all molecular ions from the MS spectra being examined by MS/MS analysis. In Fig. 9, fragmentation patterns of the selected ions *m/z* 1781, 1822, and 1794 (from spectra in Fig. 8, *A–C*, respectively) are shown. Moreover, three peaks observed in the blood group O secretor and nonsecretor samples had identical *m/z* values (1519, 1607, and 1968; Fig. 8, *A* and *C*). The fragmentation pattern showed that they corresponded to glycans of the same composition but

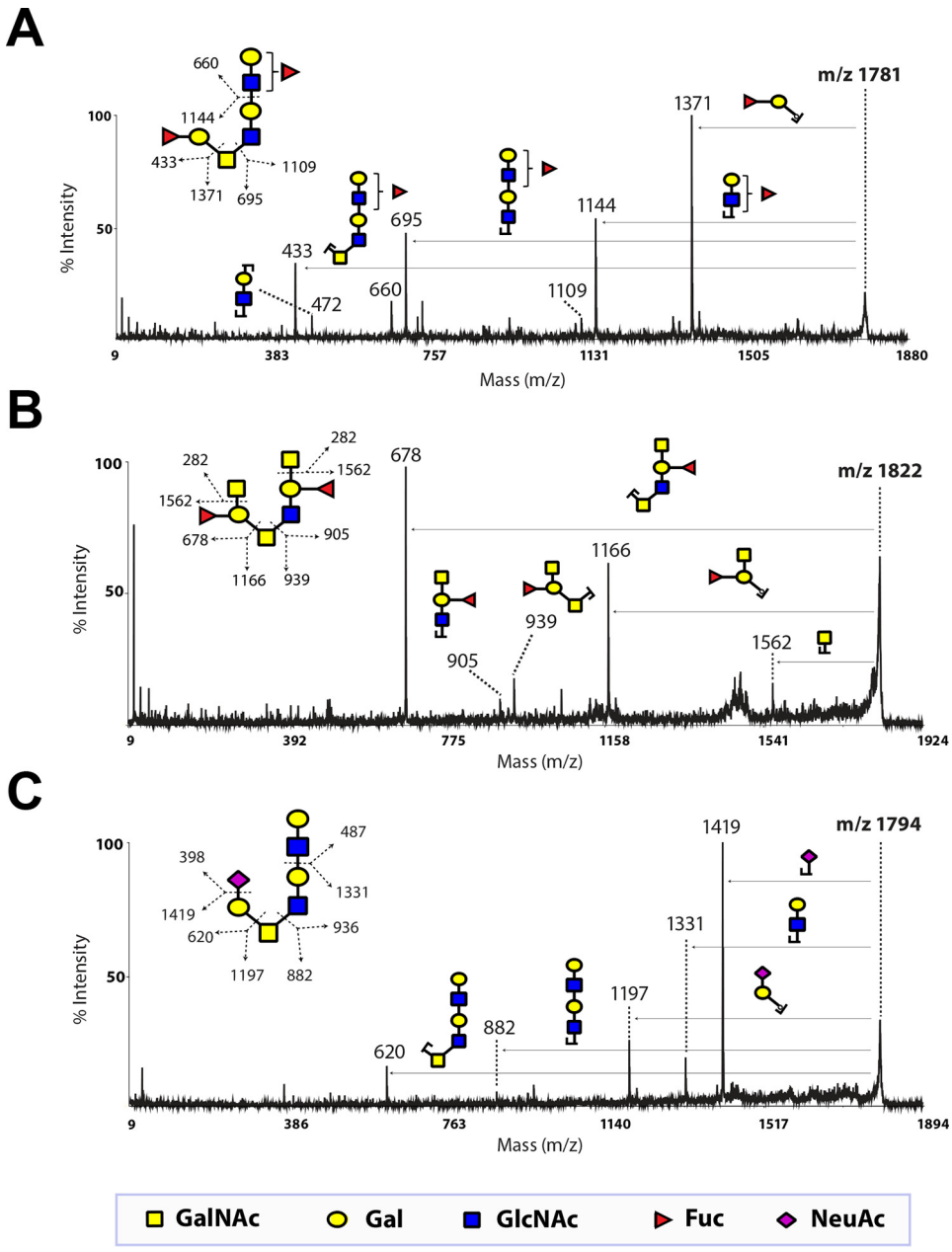

Figure 9. MALDI-TOF/TOF-MS/MS fragmentation spectra confirm the annotation of selected precursor ions from the CEL *O*-glycome. Molecular ions *m/z* 1781, 1822, and 1794 from Fig. 8, *A–C*, respectively, underwent collision-induced dissociation and the resulting fragmentation spectra are shown. *Arrows* pointing from the *dashed line* indicate the loss of a specific fragment from the precursor ion. All fragment ions are $[M+Na]^+$. When structures have not been unequivocally defined from MS/MS information, the monosaccharide is shown after a bracket.

with different architecture because of the position of the fucose residue. Such differences are exemplified in Fig. S3 where two diverging fragmentation patterns of *m/z* 1519 are shown.

Characterization of the O-glycome of recombinant CEL

After studying native CEL isolated from pancreatic juice, we asked whether *O*-glycosylation of the recombinant protein expressed in human cell lines would reflect *ABO/FUT2* status of the host cells. We started by analyzing HEK293 cells stably transfected with a CEL construct containing 16 VNTR repeats (11, 12) as this line is a commonly used system for expressing mammalian glycoproteins. Genotyping of the cells, performed as described previously (32), predicted they derived from a blood group O and *FUT2*-positive individual. Secreted CEL protein was purified and analyzed for *O*-glycans in the same way as for pancreatic juice. A relatively diverse pool of *O*-glycans was detected (Fig 10*A*) with around half of the signal intensity corresponding to core 2– based structures. No ABO blood group antigens were detected on the secreted CEL protein even though the cells were *FUT2*-positive. To verify that the detected *O*-glycans originated solely from the mucinous domain of CEL, we analyzed HEK293 cells expressing CEL-TRUNC, a construct in which a stop codon had been introduced immediately before the VNTR region (11, 12). Only two glycan peaks were detected (Fig. S4*A*). They had similar molecular mass and relative abundance as the two glycans detected in a DMEM

containing 10% FBS sample (Fig. S4*B*). This confirmed that only the mucinous domain of recombinant CEL underwent *O*-glycosylation in our model system.

Finally, we analyzed the CEL *O*-glycome after the construct had been transfected into cancer cell lines from the two major tissues of CEL expression (pancreas: MIA PaCa-2 and PANC-1 cells; breast: SK-BR-3 cells). Genotyping predicted that both pancreatic cell lines were of blood group O, with PANC-1 stemming from a *FUT2*-positive and MIA PaCa-1 from a *FUT2*-negative individual. In both lines and regardless of secretor status, only one major glycan peak corresponding to a disialylated core 2 structure (*m*/*z* 1257) was found (Fig. 10, *B* and *C*). The SK-BR-3 cell line had an A_1O genotype (= blood group A) and was *FUT2*-positive. Some core 2 structures were detected (*m*/*z* 1344, 1706, 1794, and 2156), but no H or A antigens could be seen (Fig. 10*D*). Thus, similar to the pancreatic cell lines, SK-BR-3 cells were unable to glycosylate CEL in the same selective way as seen in pancreatic juice samples.

Discussion

CEL has been linked to the autosomal dominantly inherited pancreatic syndrome MODY8 (10) and to idiopathic chronic pancreatitis (14). However, whether CEL has a role in pancreatic malignancies is still an open question. No genome-wide association studies of pancreatic cancer have so far identified any risk SNPs within or close to the *CEL* gene (33, 34). Neither the *CEL-HYB* variant (the allele predisposing for chronic pancreatitis) nor specific *CEL* VNTR lengths were enriched among pancreatic cancer cases compared with controls (8, 35). Nevertheless, the identification and characterization of FAPP, a postulated oncofetal variant of CEL with six VNTR repeats, has raised the possibility that glycoisoforms of CEL could serve as diagnostic markers or even targets for treatment in pancreatic cancer (27–29, 36).

In the current study, by using complementary techniques, we found that CEL was not detectably expressed in either neoplastic cells of PDAC tissue sections or in the pancreatic cancer cell lines examined. The only exception was BxPC-3 cells, where a weak protein band that might correspond to CEL was detected, despite the mRNA level being as low as in native HEK293 cells. Notably, BxPC-3 is a cell line derived from a moderately well-differentiated adenocarcinoma with WT *KRAS* gene (37, 38), and therefore not fully representative for PDAC tumor cells. We observed that CEL expression disappeared when acinar-to-ductal metaplasia was present, confirming that the protein is a marker of pancreatic acinar cells only when these remain polarized and in acini-like arrangement. Our results are consistent with those of Reuss and coworkers (39). When they examined 25 ductal or mucinous adenocarcinomas from the pancreas, all cases were negative for CEL mRNA by *in situ* hybridization. Notably, a single case of pancreatic acinar cell carcinoma showed slightly positive expression (39).

Our results therefore support the conclusion that CEL is unlikely to correspond to the oncofetal marker FAPP. Moreover, we find it unlikely that there is a cancer-specific number of VNTR repeats in CEL. Rather, we suggest that the SOJ-6 cell line used in previous studies either was derived from a subject with only six VNTR repeats or mutated to this repeat number because of the inherent genetic instability of cancer cells.

Because acinar pancreatic markers expressed only during embryogenesis and oncogenesis have been identified and we could not detect CEL in neoplastic tissue or cells, we wondered which antigen the anti-CEL antibody mAb16D10 did detect in pancreatic neoplastic cells (22, 23). Knowing that mAb16D10 reacts with the highly *O*-glycosylated C-terminal of CEL (28), we tested the antibody against an array of more than 600 different mammalian glycan structures. Glycans containing the blood group A antigen consistently showed the highest binding (Fig. 4). The presence of blood group antigens in the *O*-glycome of CEL was then verified directly on CEL protein isolated from pancreatic juice (Figs. 7 and 8). Based on the finding of H and A antigens attached to CEL, we assume that the protein, when isolated from blood group B individuals, will be modified by blood group B antigens, but this remains to be shown.

The samples investigated, as well as the juice sample used for mAb16D10 production, all stemmed from patients operated for pancreatic cancer. It will therefore be necessary to analyze pancreatic juice from healthy subjects to determine whether the same glycan structures are present as in our PDAC patients. Notably, aberrant glycosylation is a common characteristic for malignant transformation (40). This is in line with our observation that the examined cell lines (Fig. 10) had a generally limited capacity to *O*-glycosylate CEL and did not attach blood group antigens to the protein.

It is perhaps not surprising that CEL's mucin-like C-terminal domain contains blood group antigens. Mucinous *O*-glycans consist mostly of core 1–4 structures further elongated with lactosamine chains and terminated by fucose and sialic acid (41). Therefore, the presence of ABH or Lewis-type blood group antigens are not unusual on such proteins (42). In studies of bile salt–stimulated lipase, the milk counterpart of CEL, the threonine residues flanking the consensus sequence PVPP of the mucinous domain were proposed to carry *O*-glycans (19), and terminal Lewis antigens Le^a, Le^b, and Le^x were suggested to be present on this protein region (19, 43). Nevertheless, as far as we know, no previous study has detected blood group antigens directly on pancreatic CEL using high-sensitivity MS.

The antibody mAb16D10 also showed reactivity against Tn motifs. Truncation of the *O*-glycans in CEL and exposure of the first GalNAc residue (GalNAcα1-O-Ser/Thr) might have explained the reactivity of mAb16D10 toward both A and Tn antigens. However, in the MS analysis of purified CEL protein we did not detect any peak at *m*/*z* 330 corresponding to Tn. A peak at *m*/*z* 691 initially suggested a sialylated Tn structure (= STn antigen), but this was not consistent with the predicted glycan fragmentation pattern obtained when MS/MS was performed. Moreover, in blots of immunoprecipitates, no band matching CEL in size was seen with the anti-Tn antibody, although this antigen might be present in a higher-molecular-mass protein of ~170 kDa protein that co-precipitated with CEL (Fig. 7, *upper panel*). Taken together, we find that mAb16D10 has reactivity toward Tn, but that CEL purified

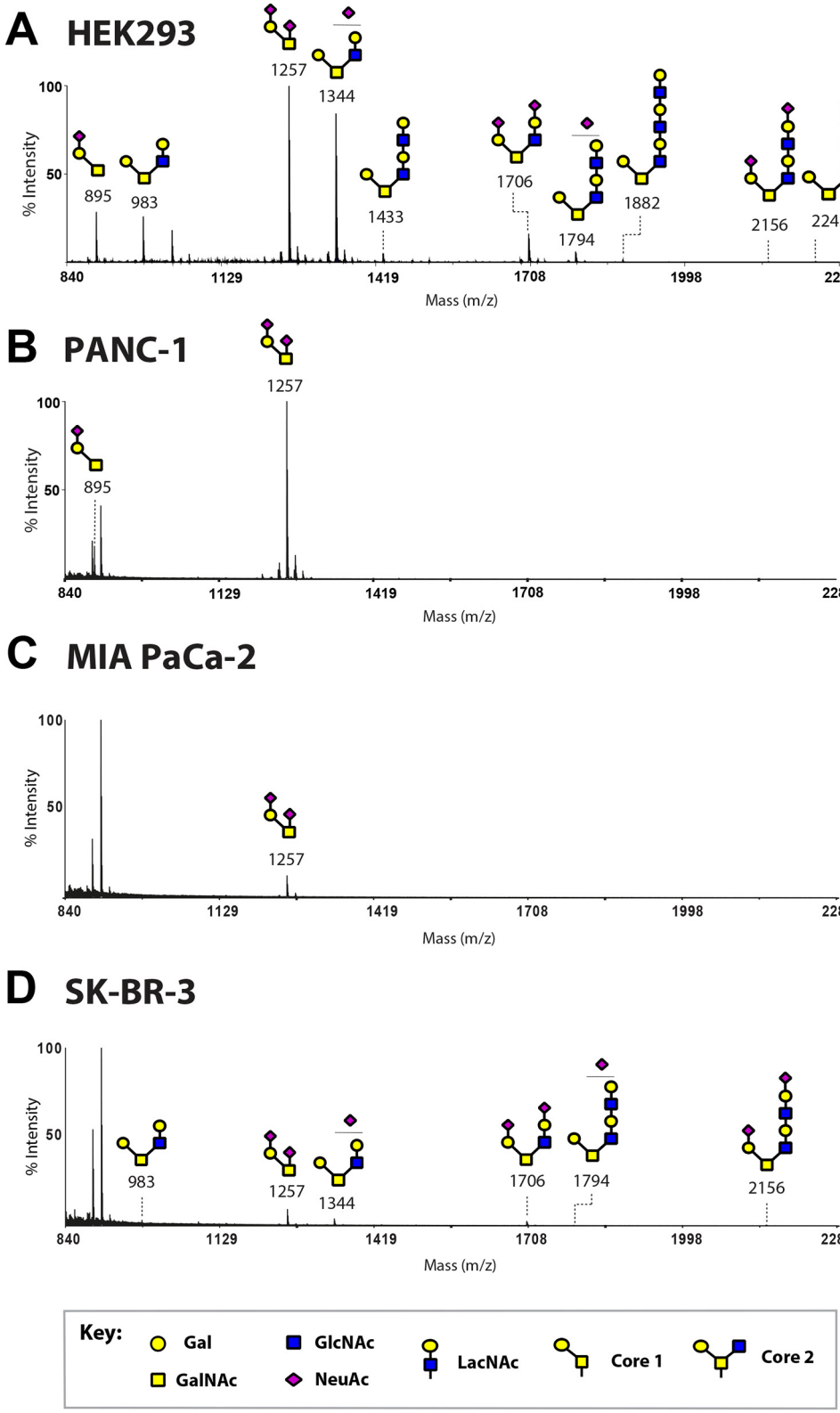

Figure 10. The *O*-glycome of recombinant CEL is dramatically altered in cancer cell lines. *A–D*, the *O*-glycan pool of recombinant CEL expressed in HEK293 (*A*), pancreatic cancer (*B*, PANC-1; *C*, MIA PaCa-2), and breast cancer (*D*, SK-BR-3) cell lines were investigated by MALDI-TOF MS after alkaline β-elimination and permethylation. The *O*-glycan population varied with the cellular expression system employed. No ABO blood group antigens were detected in any cell line. See Fig. 8 legend for further information about the spectra.

from pancreatic juice of PDAC patients does not seem to carry this antigen in detectable amounts. We speculate that the staining of mAb16D10 observed in gastric and breast cancer (Fig. S2) could be because of Tn positivity and therefore consistent with the pancarcinoma nature of this antigen (44, 45).

CEL is, in some respects, unique among digestive enzymes of the pancreas. The protein is expressed in several nonacinar cell types and has been linked to nonpancreatic pathogenic processes (*e.g.* Ref. 46). Our finding that the C-terminal mucin-like domain of CEL can be modified by blood group antigens should therefore stimulate discussions about this heavily glycosylated region and its significance for CEL function. Neither chicken nor fish CEL contain the VNTR region (47), and truncated human CEL variants (devoid of the VNTR) are enzymatically active (14, 48, 49). Thus, the C-terminal domain is clearly dispensable for the catalytic activity of the protein although a role in substrate specificity cannot be ruled out. It is conceivable that *O*-glycosylation serves to increase the stability of CEL as the C-terminal region bears amino acid similarity to protein sequences that can be a signal for proteolytic degradation (50, 51).

Another possibility is that CEL, through its C-terminal region, contributes to the mucosal barrier in the gastrointestinal tract. A main role of intestinal mucins is to provide lubrication and create a barrier that will prevent infection by the large number of microorganisms that populate the gut (52). This function is exerted through the ability of *O*-glycans to retain water and form mucus gels (53). Bearing in mind that CEL composes up to 4% of the pancreatic acinar proteins (3), the molecule could to some extent add to the gastrointestinal mucosal barrier, with the potential of interacting with intestinal microorganisms (54–56). Even the presence of blood group antigens on CEL might be understood in this perspective. In the analyzed juice samples, the identified glycan pools of CEL were fully consistent with the patients' *ABO* and *FUT*2 genotypes, with the H antigen core 1 structure being one of the most abundant motifs detected in the secretor samples. ABO blood groups are genetically determined factors that modulate the interaction between host and intestinal microbiota as well as the flora composition itself, by providing carbohydrate antigens that act as anchoring sites for commensal bacteria (54, 57).

ABO blood group status convincingly associates with risk for developing pancreatic cancer (31–33, 58). The mechanistic basis for this association remains to be explained although cross-reactivity between blood group IgM isoagglutinins with blood group–like tumor-associated carbohydrate antigens has been suggested as an explanation (59). Also for chronic pancreatitis, a study has reported that ABO blood group status, in particular the B phenotype, is a risk factor for this inflammatory condition (60, 61). However, others have found no association between ABO blood groups and chronic pancreatitis (62, 63). Moreover, *FUT2*-negative status has been linked to chronic pancreatitis (60, 61) but not to pancreatic cancer (31, 32), and it is an open question whether the inactivation of the *FUT2* gene product represents a detrimental or beneficial effect with regard to human health. In conclusion, the variability in the overall glycosylation patterns of secreted gastrointestinal proteins, including CEL, could play a role in the susceptibility to pancreatic diseases. We foresee that this will constitute an interesting topic for studies in the years to come.

Experimental procedures

Antibodies

Three different anti-CEL antibodies were used: a polyclonal rabbit antiserum (against peptide sequence 299–427 of the CEL globular domain) for immunostainings (Sigma-Aldrich, cat. HPA052701), a polyclonal rabbit antiserum for immunoblotting (generated against the truncated CEL form pV562X, recently published in Ref. 13), and the mouse mAb As20.1 for immunoprecipitation (raised against the CEL globular domain, a generous gift from Prof. Olle Hernell, Umeå University, Sweden). The antibody mAb16D10 has been described previously (27–29). Anti-Tn antibody was a generous gift from Prof. Ulla Mandel (Copenhagen University, Denmark). Mouse monoclonal anti-A (sc-69951) and goat polyclonal anti-GAPDH antibodies (sc-20357) were from Santa Cruz Biotechnology. Secondary antibodies were HRP-donkey anti-mouse (Invitrogen, cat. 626520), HRP-donkey anti-goat (Novus Biologicals, cat. NB7379), FITC-donkey anti-rabbit (Jackson ImmunoResearch Laboratories, cat. 711-095-152), and HRP-goat anti-rabbit (Invitrogen, cat. 656120) and Alexa Fluor 488 anti-mouse (Invitrogen, cat. A-10680). MACH3 anti-mouse (cat. M3M530H) or anti-rabbit HRP-conjugated polymer (cat. M3R531H) were from Biocare Medical.

Human pancreatic cancer samples

FFPE pancreatic tissue blocks from either blood group A or blood group O subjects were selected from a cohort of quality-controlled PDAC cases that had been genotyped to determine *ABO* and *FUT2* status, as described earlier (32). Pancreatic juice was obtained from patients undergoing the Whipple procedure for resection of pancreatic head tumors. After transection of the pancreas, the distal, dilated pancreatic duct was cannulated, and a sample of juice was suctioned out and stored at −80 °C immediately. cOmplete Protease Inhibitor mixture (Roche, cat. 11697498001) was added when samples were thawed for analysis. Juice samples for the study were selected based on the patients' ABO and secretor phenotype. The patients had consented to the study, which was approved by the Regional Ethical Committee of Western Norway and performed according to the Helsinki Declaration.

Cell cultures

Human pancreatic cancer cell lines (BxPC-3, MIA PaCa-2, PANC-1) and HeLa cells (CCL-2) were obtained from American Type Culture Collection (ATCC). HEK293 cells (Clontech) stably transfected with pcDNA3.1/V5-His plasmids containing either WT CEL, CEL-TRUNC, or no insert were the same as described previously (11, 12). PANC-1, HeLa, and HEK293 cells were cultured in DMEM (Sigma-Aldrich) with 500 μg Geneticin (G-418; Invitrogen), 10% FBS (Invitrogen), and 100 units/ml penicillin/streptomycin. BxPC-3 were maintained in RPMI 1640 medium (Sigma-Aldrich) supplemented with 10% FBS and 100 units/ml penicillin/streptomycin. MIA PaCa-2 cells were cultured in DMEM supplemented with 10% FBS, 2.5%

horse serum (ATCC, cat. 30-2040), and 100 units/ml penicillin/streptomycin. Human breast cancer cell line SK-BR-3 (ATCC) was grown and maintained in McCoy's 5A medium with 10% FBS and 100 units/ml penicillin/streptomycin. All cells were cultured in a standard humidified incubator at 37 °C in a 5% CO_2 atmosphere.

Electroporation of cancer cell lines

The 4D-Nucleofector instrument (Lonza) was used. One million MIA PaCa-2, PANC-1, or SK-BR-3 cells were electroporated (DN-100 or EO-137 programs) in presence of 2 μg of the CEL construct in 100 μl of SF or SE buffers (Lonza cat. V4XC-2012 and V4XC-1012). After the pulse application, the cells were incubated for 10 min in serum-free RPMI medium at 37 °C in 5% CO_2 before they were transferred to 60 mm dishes with standard growth medium. G418 was added 48 h post transfection at a concentration of 1 mg/ml. After 2–3 weeks of G418 selection, antibiotic-resistant cells were transferred to T75 flasks and maintained in 500 μg/ml G418. When cells reached 90% confluency, the growth medium containing secreted proteins was collected, filtered through 0.22-μm syringe filters, and concentrated 10 times in a vacuum concentrator. CEL was immunoprecipitated from the concentrated sample by employing the anti-CEL As20 antibody.

Immunohistochemistry

FFPE pancreatic tissue sections (3–5 μm) were placed onto SuperFrost Plus Adhesion slides (Menzel-Gläser Laboratories), dried overnight at 56 °C, deparaffinized in xylene, gradually rehydrated with decreasing concentrations of ethanol, and washed with distilled water and PBS containing Tween 0.05% (v/v). The slides were then incubated in Tris-EDTA buffer (pH 9) in a pressurized heating chamber at 120 °C for 1 min. Next, the slides were cooled down under running tap water and incubated at 4 °C overnight with the antibodies mAb16D10 (1:100 dilution), anti-A (1:2000), or anti-CEL (1:100) (Sigma-Aldrich), or for 1 h at room temperature with anti-Tn (undiluted supernatant). Blocking of endogenous peroxidase activity was done by incubating the sections in an aqueous solution of 3% hydrogen peroxide (v/v) for 5 min at room temperature. Primary antibody detection was performed with MACH3 anti-mouse or anti-rabbit HRP-conjugated polymers (Biocare Medical) using two incubations of 20 min with vigorous washing after each step on a rocking platform. Staining was visualized by developing with 3,3′-diaminobenzidine as substrate. The sections were counterstained with Mayer's hematoxylin (Dako) for 1 min and then dehydrated in alcohol, cleared in xylene, and eventually mounted with permanent mounting media.

In situ hybridization

Using a custom-made *CEL*-specific probe covering exons 2–7, the RNAscope 2.0 HD assay was employed according to the supplier's instructions (Advanced Cell Diagnostics). Briefly, after deparaffinization and rehydration, tissue sections were sequentially treated with endogenous hydrogen peroxidase block solution for 10 min at room temperature followed by an immersion in a 100 °C preheated retrieval solution for 15 min and subjected to protease digestion at 40 °C for 30 min, rinsing with distilled water after each step. The sections were then hybridized with the *CEL* probe at 40 °C for 2 h in a HybEZ oven (Advanced Cell Diagnostics). After wash buffer steps, signal detection and amplification were performed using the RNAscope 2.0 HD detection reagents (Advanced Cell Diagnostics, cat. 322310), starting with the application of the signal enhancer solutions, then washing vigorously between each step and eventually adding 3,3′-diaminobenzidine as substrate for HRP. The sections were counterstained with Mayer's hematoxylin for 1 min and then dehydrated in alcohol, cleared in xylene, and eventually mounted with permanent mounting media. Images were acquired at various magnifications using a MC170HD camera attached to a DM2000 LED microscope (Leica) and processed using Leica Application Suite V4.8 software.

When *in situ* hybridization was combined with immunofluorescence, the RNAscope 2.0 HD detection system with alkaline phosphatase (Advanced Cell Diagnostics, cat. 310036) was first used in conjugation with the VECTOR Red fluorescent substrate (Vector Laboratories, cat. SK-5100). The sections were then incubated with anti-CEL antibody (1:100) (Sigma-Aldrich) overnight, and thereafter with secondary antibody (donkey anti-rabbit IgG-FITC; 1:50) for 1 h. All washing steps were performed using TBS containing Tween 0.05% (w/v) when alkaline phosphatase was used instead of HRP. For mounting, Gold Antifade Solution with DAPI (Invitrogen) was used. Images were collected using a SP5 AOBS confocal microscope (Leica Microsystems) with 40×/1.4 NA and 63×/1.4 NA HCX Plan-Apochromat oil immersion objectives, ~1.2 airy unit pinhole aperture, and appropriate filter combinations. Images were acquired with 405 Diode and Argon ion/Argon Krypton lasers (Leica). The obtained images were merged and processed using Photoshop CC and Adobe illustrator CC (Adobe Systems).

RNA isolation and real-time quantitative PCR (RT-qPCR)

FFPE tissue sections (3–5 sections, 10 μm each) from the tumor, corresponding to either neoplastic areas or morphologically preserved pancreatic parenchyma, were scraped off from the glasses after comparison with parallel sections stained with H&E. After deparaffinization, RNA was isolated using the RNeasy FFPE Kit (Qiagen, cat. 73504) or the RNeasy Micro Kit (Qiagen, cat. 74004), according to the manufacturer's instructions. For cDNA synthesis, reverse transcription was performed on 100 ng RNA utilizing the High-Capacity cDNA Reverse Transcription Kit (Applied Biosystems/Thermo Fisher Scientific). Specific predesigned PCR primers/probe sets were purchased from Applied Biosystems (*CEL*: Hs 01068709_m1; *QARS*: Hs00192530_m1, and *GAPDH*: Hs02758991_g1 as normalizing control). RT-qPCR was performed using TaqMan Universal PCR Master Mix (Applied Biosystems, cat. 4440040) following the manufacturer´s instructions. The PCR conditions were 40 cycles of denaturation at 95 °C for 15 s followed by combined annealing/extension at 60 °C for 1 min. Fluorescent intensity was measured, and results were processed with SDS software, version 2.2 (Applied Biosystems).

Cell lysis and Western blot analyses

Pellets from cultured cells were washed with ice-cold PBS, treated with ice-cold RIPA lysis buffer (Thermo Fisher Scientific, cat. 89900) and centrifuged for 30 min at maximum speed at 4 °C. Fifteen μg of total protein was mixed with sample buffer (Life Technologies, cat. NP0007) and reducing agent (Invitrogen, cat. NP009), boiled at 90 °C for 5 min and resolved in NuPAGE Novex 7% Tris acetate gels. Separated proteins were transferred to PVDF membrane following standard protocols, then immunoblotted with polyclonal rabbit anti-CEL antibody (1:10000) (13). Staining with anti-GAPDH antibody (1:500) was used as loading control. Blots were developed using Amersham ECL Prime Western Blotting Detection Reagent (GE Healthcare Life Sciences, cat. RPN2232) and images were detected on the Syngene G:Box XR5 chemiluminescent imaging system (ISS).

Glycan arrays

An aliquot of mAb16D10 was analyzed by glycan microarray technology at the Consortium for Functional Glycomics at Emory University, Atlanta, GA. The antibody was incubated at a concentration of 50 μg/ml on a Mammalian Printed Glycan Array Version 5.2 (609 structures, available on www.functionalglycomics.org/glycomics/publicdata/primaryscreen.jsp)[4] or on a glycopeptide array (56 compounds, Table S1), and probed for binding using fluorescent Alexa Fluor 488 anti-mouse antibody (Invitrogen, cat. A-10680). On the latter array, also an anti-Tn antibody was probed. The arrays were processed using published methods (64). Binding experiments were done in replicates of six, removing the highest and lowest values from each replicate set and calculating the mean binding efficiency from the remaining four values.

Immunoprecipitation

CEL glycoprotein was purified from pancreatic juice or concentrated conditioned growth medium with the Pierce Co-Immunoprecipitation Kit (Thermo Fisher Scientific, cat. 26149) as follows: 50–400 μl pancreatic juice (protein concentration between 0.8 and 5.4 μg per μl) or 1–4 ml of medium was incubated in a spin-column containing immobilized antibody to the Agarose resin (As20.1 antibody for CEL or unspecific mouse immunoglobulin for negative control). The sealed columns were incubated overnight at 4 °C on a rotating wheel. Washing steps were performed using either PBS or RIPA buffer for immunoprecipitation (Merck Millipore, cat. 20-188), and elution was achieved using 50 mM Tris-HCl, pH 8, with 2.5% w/v SDS. Five μl eluate was separated by standard SDS-PAGE (SDS-PAGE) and immunoblotted with polyclonal rabbit anti-CEL antibody (1:10000) (13), mAb16D10 (1:100), anti-A (1:500), or anti-Tn (1:5) antibody. All incubations were done overnight at 4 °C on a rocking platform. For MS analysis, the rest of the eluted protein was subjected to SDS-PAGE electrophoresis and the resulting gel stained with Colloidal Blue Staining Kit (Thermo Fisher Scientific, cat. LC6025) and washed thoroughly with ultrapure water prior to in-gel digestion.

[4] Please note that the JBC is not responsible for the long-term archiving and maintenance of this site or any other third party hosted site.

In-gel digestion of purified glycoprotein

Excised bands corresponding to CEL were first destained in a 50% acetonitrile (MeCN) (v/v) solution in 50 mM ammonium bicarbonate for 10 min, followed by incubation in 10 mM DTT solution for 30 min at 56 °C. The gel pieces were desiccated, followed by incubation with a 55 mM solution of iodoacetic acid for 30 min in darkness at room temperature. The gel pieces were desiccated again prior to incubation with 1 μg of porcine trypsin (Sigma-Aldrich, cat. S8045) in 50 mM ammonium bicarbonate, pH 8.5 (adjusted with ammonia), overnight at 37 °C. Following extraction of the tryptic glycopeptides from the gel in 0.1% TFA/MeCN (1:2 v/v), the volume was reduced by a vacuum concentrator and the samples were freeze-dried by complete lyophilizing before proceeding to reductive elimination. All solvents used for glycan purification and analysis were HPLC-grade or higher.

Release of O-glycans by reductive elimination

O-glycans were released from the mixture of peptides/glycopeptides by reductive elimination in 400 μl of potassium borohydride (55 mg/ml in 0.1 M potassium hydroxide) at 45 °C for 16 h. After the reaction had been terminated by dropwise addition of glacial acetic acid, the mixture was passed through a Dowex beads 50W-X8 50–100 mesh (Sigma-Aldrich, cat. 217492) chromatography column and the eluate was freeze-dried. Excess borates were removed by co-evaporation with repeated addition of 10% methanolic acetic acid under a stream of nitrogen.

Permethylation of dried O-glycans

Two ml of a slurry composed of freshly crushed sodium hydroxide pellets and DMSO was added to the sample, followed by 600 μl of methyl iodide. The mixture was vigorously mixed on an automatic shaker for 45 min at room temperature. One ml of water was added to terminate the reaction, followed by another 1 ml of chloroform to recover the permethylated glycans. The aqueous phase was washed three times to remove impurities, and the chloroform layer was then dried under a nitrogen stream. Permethylated *O*-glycans were purified using a Sep-Pak Classic C18 cartridge (Waters). The cartridge was conditioned successively with methanol, water, MeCN, and water. The samples were dissolved in 1:1 (v/v) methanol-water, loaded onto the cartridge, washed with water and 15% (v/v) aqueous MeCN solution, and then eluted using a 35% (v/v) aqueous MeCN solution. The organic solvent was removed on a vacuum concentrator and samples were lyophilized overnight prior to MS analyses.

MALDI-TOF MS

MALDI-TOF MS data on permethylated samples were acquired in the reflectron positive-ion mode using a 4800 MALDI-TOF/TOF mass spectrometer (Applied Biosystems). The instrument was calibrated externally using the Calmix 4700 calibration standard, samples were dissolved in 10 μl of methanol, and 1 μl was mixed at a 1:1 ratio (v/v) with 20 mg/ml 3,4-diaminobenzophenone (DMBP) in 75% (v/v) MeCN in water as matrix. The samples were then spotted onto a 384-

well sample plate and dried at room temperature. Data were acquired using 4000 Series Explorer instrument control software and were processed using the software Data Explorer (Version 4.9, Applied Biosystems). MS spectra were assigned and annotated with the help of the GlycoWorkbench software (65). Further MS/MS analyses of peaks observed in the MS spectra were carried out using the same instrument. The potential difference between the source acceleration voltage and the collision cell was set to 1 kV, and argon was used as collision gas.

Statistical analyses

Analyses were performed using GraphPad prism 5.03 for Windows (GraphPad Software, San Diego CA).

Author contributions—K. E. J., B. B. J., K. F., D. L., A. D., E. M., and A. M. conceptualization; K. E. J., H. I., and S. M. H. data curation; K. E. J., S. M. H., and A. M. formal analysis; K. E. J., P. R. N., A. D., and A. M. funding acquisition; K. E. J., B. B. J., K. F., A. A., H. I., M. H. C., S. M. H., and A. M. investigation; K. E. J., A. A., H. I., D. H., M. E. L., A. D., E. M., S. M. H., and A. M. methodology; K. E. J. writing-original draft; K. E. J., B. B. J., K. F., A. A., H. I., M. H. C., D. H., M. E. L., D. L., P. R. N., A. D., E. M., S. M. H., and A. M. writing-review and editing; B. B. J., K. F., P. R. N., and A. M. supervision; A. A. validation; D. H., M. E. L., D. L., A. D., E. M., and A. M. resources; P. R. N. and A. M. project administration.

Acknowledgments—We thank Dong Li Lu for help in MALDI-TOF-MS and MS/MS data acquisition. We acknowledge the participation of the Protein-Glycan Interaction Resource of the Consortium for Functional Glycomics (Grant R24 GM098791) for the glycan array experiments, Ulla Mandel and Olle Hernell for providing antibodies, and Elisabeth O. Berge for providing the SK-BR-3 cell line.

References

1. Whitcomb, D. C., and Lowe, M. E. (2007) Human pancreatic digestive enzymes. *Dig. Dis. Sci.* **52,** 1–17 CrossRef Medline
2. Hernell, O., and Bläckberg, L. (1994) Human milk bile salt-stimulated lipase: Functional and molecular aspects. *J. Pediatr.* **125,** S56–S61 CrossRef Medline
3. Lombardo, D., Guy, O., and Figarella, C. (1978) Purification and characterization of a carboxyl ester hydrolase from human pancreatic juice. *Biochim. Biophys. Acta* **527,** 142–149 CrossRef Medline
4. Johansson, B. B., Fjeld, K., El Jellas, K., Gravdal, A., Dalva, M., Tjora, E., Raeder, H., Kulkarni, R. N., Johansson, S., Njølstad, P. R., and Molven, A. (2017) The role of the carboxyl ester lipase (CEL) gene in pancreatic disease. *Pancreatology* **18,** 12–19 CrossRef Medline
5. Chen, J. C., Miercke, L. J., Krucinski, J., Starr, J. R., Saenz, G., Wang, X., Spilburg, C. A., Lange, L. G., Ellsworth, J. L., and Stroud, R. M. (1998) Structure of bovine pancreatic cholesterol esterase at 1.6 A: Novel structural features involved in lipase activation. *Biochemistry* **37,** 5107–5117 CrossRef Medline
6. Torsvik, J., Johansson, S., Johansen, A., Ek, J., Minton, J., Raeder, H., Ellard, S., Hattersley, A., Pedersen, O., Hansen, T., Molven, A., and Njølstad, P. R. (2010) Mutations in the VNTR of the carboxyl-ester lipase gene (CEL) are a rare cause of monogenic diabetes. *Hum. Genet.* **127,** 55–64 CrossRef Medline
7. Lindquist, S., Bläckberg, L., and Hernell, O. (2002) Human bile salt-stimulated lipase has a high frequency of size variation due to a hypervariable region in exon 11. *Eur. J. Biochem.* **269,** 759–767 CrossRef Medline
8. Dalva, M., El Jellas, K., Steine, S. J., Johansson, B. B., Ringdal, M., Torsvik, J., Immervoll, H., Hoem, D., Laemmerhirt, F., Simon, P., Lerch, M. M., Johansson, S., Njølstad, P. R., Weiss, F. U., Fjeld, K., and Molven, A. (2017) Copy number variants and VNTR length polymorphisms of the carboxyl-ester lipase (CEL) gene as risk factors in pancreatic cancer. *Pancreatology* **17,** 83–88 CrossRef Medline
9. Ragvin, A., Fjeld, K., Weiss, F. U., Torsvik, J., Aghdassi, A., Mayerle, J., Simon, P., Njølstad, P. R., Lerch, M. M., Johansson, S., and Molven, A. (2013) The number of tandem repeats in the carboxyl-ester lipase (CEL) gene as a risk factor in alcoholic and idiopathic chronic pancreatitis. *Pancreatology* **13,** 29–32 CrossRef Medline
10. Raeder, H., Johansson, S., Holm, P. I., Haldorsen, I. S., Mas, E., Sbarra, V., Nermoen, I., Eide, S. A., Grevle, L., Bjørkhaug, L., Sagen, J. V., Aksnes, L., Søvik, O., Lombardo, D., Molven, A., and Njølstad, P. R. (2006) Mutations in the CEL VNTR cause a syndrome of diabetes and pancreatic exocrine dysfunction. *Nat. Genet.* **38,** 54–62 CrossRef Medline
11. Johansson, B. B., Torsvik, J., Bjørkhaug, L., Vesterhus, M., Ragvin, A., Tjora, E., Fjeld, K., Hoem, D., Johansson, S., Raeder, H., Lindquist, S., Hernell, O., Cnop, M., Saraste, J., Flatmark, T., Molven, A., and Njølstad, P. R. (2011) Diabetes and pancreatic exocrine dysfunction due to mutations in the carboxyl ester lipase gene-maturity onset diabetes of the young (CEL-MODY): a protein misfolding disease. *J. Biol. Chem.* **286,** 34593–34605 CrossRef Medline
12. Torsvik, J., Johansson, B. B., Dalva, M., Marie, M., Fjeld, K., Johansson, S., Bjørkøy, G., Saraste, J., Njølstad, P. R., and Molven, A. (2014) Endocytosis of secreted carboxyl ester lipase in a syndrome of diabetes and pancreatic exocrine dysfunction. *J. Biol. Chem.* **289,** 29097–29111 CrossRef Medline
13. Xiao, X., Jones, G., Sevilla, W. A., Stolz, D. B., Magee, K. E., Haughney, M., Mukherjee, A., Wang, Y., and Lowe, M. E. (2016) A carboxyl ester lipase (CEL) mutant causes chronic pancreatitis by forming intracellular aggregates that activate apoptosis. *J. Biol. Chem.* **291,** 23224–23236 CrossRef Medline
14. Fjeld, K., Weiss, F. U., Lasher, D., Rosendahl, J., Chen, J. M., Johansson, B. B., Kirsten, H., Ruffert, C., Masson, E., Steine, S. J., Bugert, P., Cnop, M., Grützmann, R., Mayerle, J., Mössner, J., *et al.* (2015) A recombined allele of the lipase gene CEL and its pseudogene CELP confers susceptibility to chronic pancreatitis. *Nat. Genet.* **47,** 518–522 CrossRef Medline
15. Molven, A., Fjeld, K., and Lowe, M. E. (2016) Lipase genetic variants in chronic pancreatitis: When the end is wrong, all's not well. *Gastroenterology* **150,** 1515–1518 CrossRef Medline
16. Baba, T., Downs, D., Jackson, K. W., Tang, J., and Wang, C. S. (1991) Structure of human milk bile salt activated lipase. *Biochemistry* **30,** 500–510 CrossRef Medline
17. Mechref, Y., Chen, P., and Novotny, M. V. (1999) Structural characterization of the N-linked oligosaccharides in bile salt-stimulated lipase originated from human breast milk. *Glycobiology* **9,** 227–234 CrossRef Medline
18. Sugo, T., Mas, E., Abouakil, N., Endo, T., Escribano, M. J., Kobata, A., and Lombardo, D. (1993) The structure of N-linked oligosaccharides of human pancreatic bile-salt-dependent lipase. *Eur. J. Biochem.* **216,** 799–805 CrossRef Medline
19. Wang, C. S., Dashti, A., Jackson, K. W., Yeh, J. C., Cummings, R. D., and Tang, J. (1995) Isolation and characterization of human milk bile salt-activated lipase C-tail fragment. *Biochemistry* **34,** 10639–10644 CrossRef Medline
20. Hanisch, F. G. (2001) *O*-glycosylation of the mucin type. *Biol. Chem.* **382,** 143–149 CrossRef Medline
21. Dube, D. H., and Bertozzi, C. R. (2005) Glycans in cancer and inflammation—potential for therapeutics and diagnostics. *Nat. Rev. Drug Discov.* **4,** 477–488 CrossRef Medline
22. Escribano, M. J., Carré-Llopis, A., and Loridon-Rosa, B. (1985) Expression of oncofoetal pancreatic antigens in hamster adult pancreas during experimental carcinogenesis. *Br. J. Cancer* **51,** 187–193 CrossRef Medline
23. Escribano, M. J., Cordier, J., Nap, M., Ten Kate, F. J., and Burtin, P. (1986) Differentiation antigens in fetal human pancreas. Reexpression in cancer. *Int. J. Cancer* **38,** 155–160 CrossRef Medline
24. Albers, G. H., Escribano, M. J., Gonzalez, M., Mulliez, N., and Nap, M. (1987) Fetoacinar pancreatic protein in the developing human pancreas. *Differentiation* **34,** 210–215 CrossRef Medline
25. Albers, G. H., Escribano, M. J., Daher, N., and Nap, M. (1990) An immunohistologic study of the feto-acinar pancreatic protein (FAP) in the normal pancreas, chronic pancreatitis, pancreatic adenocarcinoma, and in-

traabdominal metastases of adenocarcinomas. *Am. J. Clin. Pathol.* **93,** 14–19 CrossRef Medline
26. Mas, E., Abouakil, N., Roudani, S., Miralles, F., Guy-Crotte, O., Figarella, C., Escribano, M. J., and Lombardo, D. (1993) Human fetoacinar pancreatic protein: An oncofetal glycoform of the normally secreted pancreatic bile-salt-dependent lipase. *Biochem. J.* **289,** 609–615 CrossRef Medline
27. Crescence, L., Beraud, E., Sbarra, V., Bernard, J. P., Lombardo, D., and Mas, E. (2012) Targeting a novel onco-glycoprotein antigen at tumoral pancreatic cell surface by mAb16D10 induces cell death. *J. Immunol.* **189,** 3386–3396 CrossRef Medline
28. Panicot-Dubois, L., Aubert, M., Franceschi, C., Mas, E., Silvy, F., Crotte, C., Bernard, J. P., Lombardo, D., and Sadoulet, M. O. (2004) Monoclonal antibody 16D10 to the C-terminal domain of the feto-acinar pancreatic protein binds to membrane of human pancreatic tumoral SOJ-6 cells and inhibits the growth of tumor xenografts. *Neoplasia* **6,** 713–724 CrossRef Medline
29. Benkoël, L., Bernard, J. P., Payan-Defais, M. J., Crescence, L., Franceschi, C., Delmas, M., Ouaissi, M., Sastre, B., Sahel, J., Benoliel, A. M., Bongrand, P., Silvy, F., Gauthier, L., Romagné, F., Lombardo, D., and Mas, E. (2009) Monoclonal antibody 16D10 to the COOH-terminal domain of the feto-acinar pancreatic protein targets pancreatic neoplastic tissues. *Mol. Cancer Ther.* **8,** 282–291 CrossRef Medline
30. Mas, E., Abouakil, N., Roudani, S., Franc, J. L., Montreuil, J., and Lombardo, D. (1993) Variation of the glycosylation of human pancreatic bile-salt-dependent lipase. *Eur. J. Biochem.* **216,** 807–812 CrossRef Medline
31. Wolpin, B. M., Kraft, P., Xu, M., Steplowski, E., Olsson, M. L., Arslan, A. A., Bueno-de-Mesquita, H. B., Gross, M., Helzlsouer, K., Jacobs, E. J., LaCroix, A., Petersen, G., Stolzenberg-Solomon, R. Z., Zheng, W., Albanes, D., *et al.* (2010) Variant ABO blood group alleles, secretor status, and risk of pancreatic cancer: Results from the pancreatic cancer cohort consortium. *Cancer Epidemiol. Biomarkers Prev.* **19,** 3140–3149 CrossRef Medline
32. El Jellas, K., Hoem, D., Hagen, K. G., Kalvenes, M. B., Aziz, S., Steine, S. J., Immervoll, H., Johansson, S., and Molven, A. (2017) Associations between ABO blood groups and pancreatic ductal adenocarcinoma: influence on resection status and survival. *Cancer Med.* **6,** 1531–1540 CrossRef Medline
33. Wolpin, B. M., Rizzato, C., Kraft, P., Kooperberg, C., Petersen, G. M., Wang, Z., Arslan, A. A., Beane-Freeman, L., Bracci, P. M., Buring, J., Canzian, F., Duell, E. J., Gallinger, S., Giles, G. G., Goodman, G. E., *et al.* (2014) Genome-wide association study identifies multiple susceptibility loci for pancreatic cancer. *Nat. Genet.* **46,** 994–1000 CrossRef Medline
34. Childs, E. J., Mocci, E., Campa, D., Bracci, P. M., Gallinger, S., Goggins, M., Li, D., Neale, R. E., Olson, S. H., Scelo, G., Amundadottir, L. T., Bamlet, W. R., Bijlsma, M. F., Blackford, A., Borges, M., *et al.* (2015) Common variation at 2p13.3, 3q29, 7p13 and 17q25.1 associated with susceptibility to pancreatic cancer. *Nat. Genet.* **47,** 911–916 CrossRef Medline
35. Shindo, K., Yu, J., Suenaga, M., Fesharakizadeh, S., Tamura, K., Almario, J. A. N., Brant, A., Borges, M., Siddiqui, A., Datta, L., Wolfgang, C. L., Hruban, R. H., Klein, A. P., and Goggins, M. (2017) Lack of association between the pancreatitis risk allele CEL-HYB and pancreatic cancer. *Oncotarget* **8,** 50824–50831 CrossRef Medline
36. Martinez, E., Crenon, I., Silvy, F., Del Grande, J., Mougel, A., Barea, D., Fina, F., Bernard, J. P., Ouaissi, M., Lombardo, D., and Mas, E. (2017) Expression of truncated bile salt-dependent lipase variant in pancreatic pre-neoplastic lesions. *Oncotarget* **8,** 536–551 CrossRef Medline
37. Tan, M. H., Nowak, N. J., Loor, R., Ochi, H., Sandberg, A. A., Lopez, C., Pickren, J. W., Berjian, R., Douglass, H. O., Jr., and Chu, T. M. (1986) Characterization of a new primary human pancreatic tumor line. *Cancer Invest.* **4,** 15–23 CrossRef Medline
38. Deer, E. L., González-Hernández, J., Coursen, J. D., Shea, J. E., Ngatia, J., Scaife, C. L., Firpo, M. A., and Mulvihill, S. J. (2010) Phenotype and genotype of pancreatic cancer cell lines. *Pancreas* **39,** 425–435 CrossRef Medline
39. Reuss, R., Aberle, S., Klingel, K., Sauter, M., Greschniok, A., Franke, F. E., Padberg, W., and Blin, N. (2006) The expression of the carboxyl ester lipase gene in pancreas and pancreatic adenocarcinomas. *Int. J. Oncol.* **29,** 649–654 Medline
40. Stowell, S. R., Ju, T., and Cummings, R. D. (2015) Protein glycosylation in cancer. *Ann. Rev. Pathol.* **10,** 473–510 CrossRef Medline
41. Stanley, P., and Cummings, R. D. (2017) Structures common to different glycans. in *Essentials of Glycobiology* (Varki, A., Cummings, R. D., Esko, J. D., *et al.*, eds) 3rd ed., pp. 161–178, Cold Spring Harbor Laboratory Press, Cold Spring Harbor, NY CrossRef Medline
42. Rossez, Y., Maes, E., Lefebvre Darroman, T., Gosset, P., Ecobichon, C., Joncquel Chevalier Curt, M., Boneca, I. G., Michalski, J. C., and Robbe-Masselot, C. (2012) Almost all human gastric mucin *O*-glycans harbor blood group A, B or H antigens and are potential binding sites for *Helicobacter pylori*. *Glycobiology* **22,** 1193–1206 CrossRef Medline
43. Landberg, E., Påhlsson, P., Krotkiewski, H., Strömqvist, M., Hansson, L., and Lundblad, A. (1997) Glycosylation of bile-salt-stimulated lipase from human milk: Comparison of native and recombinant forms. *Arch. Biochem. Biophys.* **344,** 94–102 CrossRef Medline
44. Ju, T., Wang, Y., Aryal, R. P., Lehoux, S. D., Ding, X., Kudelka, M. R., Cutler, C., Zeng, J., Wang, J., Sun, X., Heimburg-Molinaro, J., Smith, D. F., and Cummings, R. D. (2013) Tn and sialyl-Tn antigens, aberrant *O*-glycomics as human disease markers. *Proteomics* **7,** 618–631 CrossRef Medline
45. Springer, G. F., Desai, P. R., Ghazizadeh, M., and Tegtmeyer, H. (1995) T/Tn pancarcinoma autoantigens: Fundamental, diagnostic, and prognostic aspects. *Cancer Detect. Prevent.* **19,** 173–182 Medline
46. Kodvawala, A., Ghering, A. B., Davidson, W. S., and Hui, D. Y. (2005) Carboxyl ester lipase expression in macrophages increases cholesteryl ester accumulation and promotes atherosclerosis. *J. Biol. Chem.* **280,** 38592–38598 CrossRef Medline
47. Holmes, R. S., and Cox, L. A. (2011) Comparative structures and evolution of vertebrate carboxyl ester lipase (CEL) genes and proteins with a major role in reverse cholesterol transport. *Cholesterol* **2011**, 781643 CrossRef Medline
48. Hansson, L., Bläckberg, L., Edlund, M., Lundberg, L., Strömqvist, M., and Hernell, O. (1993) Recombinant human milk bile salt-stimulated lipase. Catalytic activity is retained in the absence of glycosylation and the unique proline-rich repeats. *J. Biol. Chem.* **268,** 26692–26698 Medline
49. Downs, D., Xu, Y. Y., Tang, J., and Wang, C. S. (1994) Proline-rich domain and glycosylation are not essential for the enzymic activity of bile salt-activated lipase. Kinetic studies of T-BAL, a truncated form of the enzyme, expressed in *Escherichia coli*. *Biochemistry* **33,** 7979–7985 CrossRef Medline
50. Rogers, S., Wells, R., and Rechsteiner, M. (1986) Amino acid sequences common to rapidly degraded proteins: The PEST hypothesis. *Science* **234,** 364–368 Medline
51. Loomes, K. M., Senior, H. E., West, P. M., and Roberton, A. M. (1999) Functional protective role for mucin glycosylated repetitive domains. *Eur. J. Biochem.* **266,** 105–111 CrossRef Medline
52. McGuckin, M. A., Lindén, S. K., Sutton, P., and Florin, T. H. (2011) Mucin dynamics and enteric pathogens. *Nat. Rev. Microbiol.* **9,** 265–278 CrossRef Medline
53. Bergstrom, K. S. B., and Xia, L. (2013) Mucin-type *O*-glycans and their roles in intestinal homeostasis. *Glycobiology* **23,** 1026–1037 CrossRef Medline
54. Tailford, L. E., Crost, E. H., Kavanaugh, D., and Juge, N. (2015) Mucin glycan foraging in the human gut microbiome. *Front. Genet.* **6,** 81 CrossRef Medline
55. Marionneau, S., Ruvoën, N., Le Moullac-Vaidye, B., Clement, M., Cailleau-Thomas, A., Ruiz-Palacois, G., Huang, P., Jiang, X., and Le Pendu, J. (2002) Norwalk virus binds to histo-blood group antigens present on gastroduodenal epithelial cells of secretor individuals. *Gastroenterology* **122,** 1967–1977 CrossRef Medline
56. Ruvoën-Clouet, N., Mas, E., Marionneau, S., Guillon, P., Lombardo, D., and Le Pendu, J. (2006) Bile-salt-stimulated lipase and mucins from milk of 'secretor' mothers inhibit the binding of Norwalk virus capsids to their carbohydrate ligands. *Biochem. J.* **393,** 627–634 CrossRef Medline
57. Mäkivuokko, H., Lahtinen, S. J., Wacklin, P., Tuovinen, E., Tenkanen, H., Nikkilä, J., Björklund, M., Aranko, K., Ouwehand, A. C., and Mättö, J. (2012) Association between the ABO blood group and the human intes-

tinal microbiota composition. *BMC Microbiol.* **12,** 94–94 CrossRef Medline

58. Amundadottir, L., Kraft, P., Stolzenberg-Solomon, R. Z., Fuchs, C. S., Petersen, G. M., Arslan, A. A., Bueno-de-Mesquita, H. B., Gross, M., Helzlsouer, K., Jacobs, E. J., LaCroix, A., Zheng, W., Albanes, D., Bamlet, W., Berg, C. D., *et al.* (2009) Genome-wide association study identifies variants in the ABO locus associated with susceptibility to pancreatic cancer. *Nat. Genet.* **41,** 986–990 CrossRef Medline
59. Hofmann, B. T., Stehr, A., Dohrmann, T., Gungor, C., Herich, L., Hiller, J., Harder, S., Ewald, F., Gebauer, F., Tachezy, M., Precht, C., Izbicki, J. R., Bockhorn, M., Wagener, C., and Wolters-Eisfeld, G. (2014) ABO blood group IgM isoagglutinins interact with tumor-associated *O*-glycan structures in pancreatic cancer. *Clin. Cancer Res.* **20,** 6117–6126 CrossRef Medline
60. Weiss, F. U., Schurmann, C., Guenther, A., Ernst, F., Teumer, A., Mayerle, J., Simon, P., Völzke, H., Radke, D., Greinacher, A., Kuehn, J. P., Zenker, M., Völker, U., Homuth, G., and Lerch, M. M. (2015) Fucosyltransferase 2 (FUT2) non-secretor status and blood group B are associated with elevated serum lipase activity in asymptomatic subjects, and an increased risk for chronic pancreatitis: A genetic association study. *Gut* **64,** 646–656 CrossRef Medline
61. Weiss, F. U., Schurmann, C., Teumer, A., Mayerle, J., Simon, P., Völzke, H., Greinacher, A., Kuehn, J. P., Zenker, M., Völker, U., Homuth, G., and Lerch, M. M. (2016) ABO blood type B and fucosyltransferase 2 non-secretor status as genetic risk factors for chronic pancreatitis. *Gut* **65,** 353–354 CrossRef Medline
62. Greer, J. B., LaRusch, J., Brand, R. E., O'Connell, M. R., Yadav, D., Whitcomb, D. C., and NAPS2 Study Group (2011) ABO blood group and chronic pancreatitis risk in the NAPS2 cohort. *Pancreas* **40,** 1188–1194 CrossRef Medline
63. Kirsten, H., Scholz, M., Kovacs, P., Grallert, H., Peters, A., Strauch, K., Frank, J., Rietschel, M., Nöthen, M. M., Witt, H., and Rosendahl, J. (2016) Genetic variants of lipase activity in chronic pancreatitis. *Gut* **65,** 184–185 CrossRef Medline
64. Blixt, O., Head, S., Mondala, T., Scanlan, C., Huflejt, M. E., Alvarez, R., Bryan, M. C., Fazio, F., Calarese, D., Stevens, J., Razi, N., Stevens, D. J., Skehel, J. J., van Die, I., Burton, D. R., Wilson, I. A., Cummings, R., Bovin, N., Wong, C.-H., and Paulson, J. C. (2004) Printed covalent glycan array for ligand profiling of diverse glycan binding proteins. *Proc. Natl. Acad. Sci. U.S.A.* **101,** 17033–17038 CrossRef Medline
65. Ceroni, A., Maass, K., Geyer, H., Geyer, R., Dell, A., and Haslam, S. M. (2008) GlycoWorkbench: A tool for the computer-assisted annotation of mass spectra of glycans. *J. Proteome Res.* **7,** 1650–1659 CrossRef Medline
66. Varki, A., Cummings, R. D., Esko, J. D., Freeze, H. H., Stanley, P., Marth, J. D., Bertozzi, C. R., Hart, G. W., and Etzler, M. E. (2009) Symbol nomenclature for glycan representation. *Proteomics* **9,** 5398–5399 CrossRef Medline

The mucinous domain of pancreatic carboxyl-ester lipase (CEL) contains core 1/core 2 *O*-glycans that can be modified by ABO blood group determinants

Khadija El Jellas, Bente B. Johansson, Karianne Fjeld, Aristotelis Antonopoulos, Heike Immervoll, Man H. Choi, Dag Hoem, Mark E. Lowe, Dominique Lombardo, Pål R. Njølstad, Anne Dell, Eric Mas, Stuart M. Haslam and Anders Molven

J. Biol. Chem. 2018, 293:19476-19491.
doi: 10.1074/jbc.RA118.001934 originally published online October 12, 2018